

**Development of and Proposed Applications for Tetrodes in Functional  
Mapping of Rodent Sensorimotor Striatum**

by

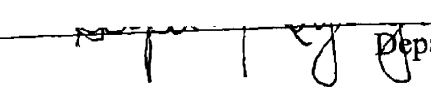
Deepa Radhakrishna Iyengar  
B.A., Physics and Astronomy (1995)  
Carleton College

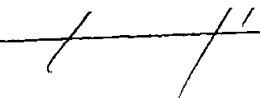
Submitted to the Department of Brain and Cognitive Sciences  
in Partial Fulfillment of the Requirements for the Degree of

Master of Science in Brain and Cognitive Sciences  
at the  
Massachusetts Institute of Technology

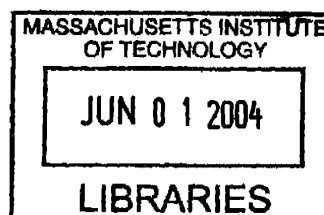
June 2004

©2004 Massachusetts Institute of Technology  
All rights reserved

Signature of Author  Department of Brain and Cognitive Sciences  
May 24, 2004

Certified and Accepted by  Earl Miller  
Picower Professor of Neuroscience  
Thesis Supervisor  
Chairman, Department Committee on Graduate Students

ARCHIVES



# **Development of and Proposed Applications for Tetrodes in Functional Mapping of Rodent Sensorimotor Striatum**

by

Deepa Radhakrishna Iyengar

Submitted to the Department of Brain and Cognitive Sciences  
on May 24, 2004 in partial fulfillment of the  
requirements for the degree of Master of Science in  
Brain and Cognitive Sciences

## **Abstract**

The Wilson-McNaughton tetrode preparation for awake, behaving rodents was adapted by a group of investigators for use in dorsolateral striatum. Measures were taken to improve the reliability of reaching the target area in the brain and the stability of the implanted tetrode drive over several weeks of recording. Novel methods were developed to confirm the dorsoventral level of tetrodes at intermediate stages of advancement during recording, and to reconstruct estimated directions and distances of recorded sources from tetrodes by post-hoc analysis. Alternative methods of source separation and data visualization were implemented. Additional refinements to improve unit separation within and across recording sessions are proposed. The resulting recording technique is expected to have considerable potential in clarifying behavioral and other functional correlates of systems of striatal anatomical compartmentalization. A set of experiments is proposed to investigate how dorsolateral striatal neuronal activity changes in correlation with learning of three stimulus-response tasks relative to three control tasks with similar sensory, motor and motivational aspects but different learning and memory requirements, and to localize task-responsive units with respect to striosomes and body part areas identified by neuronal responses to cutaneous stimulation/passive manipulation and anterograde anatomical tracers from primary motor cortex. Neuronal activity in the globus pallidus and substantia nigra pars reticulata, output areas of the basal ganglia, is also to be examined over the course of acquisition of the three stimulus-response tasks. The proposed investigations will begin to empirically anchor learning and memory functions of the striatum and basal ganglia to patterns of neuronal activity in the context of the intricate anatomical organization of these areas.

Thesis Supervisor: Earl Miller

Title: Picower Professor of Neuroscience

## Acknowledgements

I would like to express my gratitude to Kelvin Chin for his invaluable advice and guidance throughout the thesis process, without which I would not be at the point of writing acknowledgements.

Warm thanks to Denise Heintze for patiently and efficiently dealing with all the long-distance organizational issues and for her friendly support.

I am grateful to Professor Earl Miller for making it possible for me to submit a thesis, and for acting as my advisor. Thanks also to Professor Matthew Wilson for serving as an additional reader.

I am greatly indebted to Professor Vilhjálmur Kjartansson of the University of Iceland for electronics discussions which greatly clarified my discussion of tetrode methods in the first half of the paper.

With great affection I thank my family for their loving support of my efforts: Mom (Geetha), Dad (Radhakrishna), my brother Rajeev, and my parents-in-law Guðrún and Villi.

I don't know how to thank my husband Hannes for his unflagging personal and academic enthusiasm for and support of my work here and elsewhere. (Less helpful are his suggestions for phrasing this particular acknowledgement, which include usages of words like "adulation," "devotion," and "worship.")

Thanks to many friends including Dotty Guild, Deepika Gundanna, and Silver Moon Perillo for their friendly interest and support.

Fond thanks to George for dropping by for frequent visits and afternoon snacks.



This thesis is in memory of all the Freds and Axels who served as experimental subjects for this work. It must be remembered that the deaths of living beings like these lie at the center of the vortex of scholarly and careerist hopes in this field.

|            |   |           |
|------------|---|-----------|
| <b>1</b>   | <b>INTRODUCTION.....</b>  | <b>7</b>  |
| <b>2</b>   | <b>STRIATAL COMPARTMENTS AND NEURONAL TYPES .....</b>                     | <b>7</b>  |
| <b>3</b>   | <b>ADAPTATION OF TETRODES FOR STUDY OF RODENT STRIATUM.....</b>           | <b>13</b> |
| <b>3.1</b> | <b>Technical needs of a striatal extracellular recording system .....</b> | <b>13</b> |
| <b>3.2</b> | <b>Wilson-McNaughton tetrode recording system .....</b>                   | <b>16</b> |
| 3.2.1      | Manufacture and deployment of tetrodes.....                               | 16        |
| 3.2.2      | Preamplifier stage .....  | 17        |
| 3.2.3      | Amplifier, A/D converter, and data acquisition stages.....                | 19        |
| 3.2.4      | Data analysis .....   | 19        |
| <b>3.3</b> | <b>Modifications for use of tetrodes in striatum .....</b>                | <b>19</b> |
| 3.3.1      | Tetrode manufacture.....  | 19        |
| 3.3.2      | Drive manufacture .....   | 20        |
| 3.3.3      | In-vivo tetrode localization by MRI.....                                  | 20        |
| 3.3.4      | Data visualization and clustering .....                                   | 21        |
| 3.3.4.1    | Elimination of EMG noise and non-MSN spikes .....                         | 21        |
| 3.3.4.2    | Generation of power measures for clustering .....                         | 22        |
| 3.3.4.3    | Three-dimensional display of power measures .....                         | 23        |
| 3.3.4.4    | Automated clustering by K-means.....                                      | 24        |
| 3.3.4.5    | Post-hoc testing and adjustments .....                                    | 25        |
| 3.3.4.6    | Clustering by K-means versus human operators .....                        | 25        |
| 3.3.4.7    | Clustering by power measures versus peak-to-peak voltage.....             | 26        |
| 3.3.5      | Reconstruction of source locations .....                                  | 26        |
| 3.3.5.1    | Determination of source position .....                                    | 26        |
| <b>3.4</b> | <b>Experimental results.....</b>  | <b>29</b> |
| <b>3.5</b> | <b>Suggestions for further work.....</b>                                  | <b>30</b> |
| 3.5.1      | Mass production of tetrodes .....   | 30        |
| 3.5.2      | Additional clustering parameters .....                                    | 30        |
| 3.5.3      | Clustering algorithm .....  | 30        |
| 3.5.3.1    | K-means caveats .....   | 30        |
| 3.5.3.2    | Alternative clustering algorithms .....                                   | 31        |
| 3.5.3.3    | Overlapping spikes and tetrode drift.....                                 | 31        |
| 3.5.4      | Isolation of unit firing across multiple days .....                       | 32        |
| <b>3.6</b> | <b>Summary.....</b>   | <b>32</b> |

|            |  |           |
|------------|--|-----------|
| <b>4</b>   | <b>RELATING STRIATAL LEARNING TO ANATOMY: A PROPOSAL .....</b> | <b>33</b> |
| <b>4.1</b> | <b>Background .....</b>  | <b>33</b> |
| <b>4.2</b> | <b>Specific Aims .....</b>                                     | <b>40</b> |
| <b>4.3</b> | <b>Experimental design and methods.....</b>                    | <b>40</b> |
| 4.3.1      | Task designs.....  | 40        |
| 4.3.2      | Task-specific methods .....                                    | 43        |
| 4.3.2.1    | Cued and delayed alternation T-maze tasks.....                 | 43        |
| 4.3.2.2    | Cued and delayed alternation lever-press tasks .....           | 44        |
| 4.3.2.3    | Cued and delayed alternation head movement tasks .....         | 45        |
| 4.3.3      | Aim 1: experiments 1, 3, 5 .....                               | 46        |
| 4.3.3.1    | Hypothesis .....   | 46        |
| 4.3.3.2    | Design .....   | 46        |
| 4.3.3.3    | Methods .....  | 47        |
| 4.3.3.4    | Expected results .....   | 48        |
| 4.3.4      | Aims 2 and 4: experiments 2A, 4A, 6A.....                      | 48        |
| 4.3.4.1    | Hypotheses.....  | 48        |
| 4.3.4.2    | Design .....   | 48        |
| 4.3.4.3    | Methods .....  | 49        |
| 4.3.4.4    | Expected results .....   | 52        |
| 4.3.5      | Aims 3 and 4: experiments 2B, 4B, 6B.....                      | 52        |
| 4.3.5.1    | Hypotheses.....  | 52        |
| 4.3.5.2    | Design .....   | 52        |
| 4.3.5.3    | Methods .....  | 53        |
| 4.3.5.4    | Expected results .....   | 53        |
| 4.3.6      | Aim 5: experiments 2C, 4C, 6C .....                            | 53        |
| 4.3.6.1    | Hypothesis .....   | 53        |
| 4.3.6.2    | Design .....   | 53        |
| 4.3.6.3    | Methods .....  | 54        |
| 4.3.6.4    | Expected results .....   | 54        |
| 4.3.7      | Aim 6: experiments 4D and 6D.....                              | 54        |
| 4.3.7.1    | Hypothesis .....   | 54        |
| 4.3.7.2    | Design .....   | 54        |
| 4.3.7.3    | Methods .....  | 55        |
| 4.3.7.4    | Expected results .....   | 55        |
| 4.3.8      | Aim 7: experiments 7A, 8A, 9A .....                            | 55        |
| 4.3.8.1    | Hypothesis .....   | 55        |
| 4.3.8.2    | Design .....   | 56        |
| 4.3.8.3    | Methods .....  | 56        |
| 4.3.8.4    | Expected results .....   | 56        |
| 4.3.9      | Aim 7: experiments 7B, 8B, 9B .....                            | 56        |
| 4.3.9.1    | Hypothesis .....   | 56        |
| 4.3.9.2    | Design .....   | 56        |
| 4.3.9.3    | Methods .....  | 57        |
| 4.3.9.4    | Expected results .....   | 57        |

|            |  |           |
|------------|--|-----------|
| <b>4.4</b> | <b>Suggestions for further work.....</b>                               | <b>57</b> |
| <b>5</b>   | <b>CONCLUSION .....</b>  | <b>58</b> |
|            | <b>APPENDIX: FINDING C, THE SPATIAL RECONSTRUCTION PARAMETER .....</b> | <b>59</b> |
|            | <b>REFERENCES .....</b>  | <b>60</b> |

# 1 Introduction

The large and disparate variety of functionalities attributed to the basal ganglia, some of them difficult to define precisely, have resulted in the compilation of a rich body of work relating to anatomical and neurochemical aspects of these nuclei. Less intelligible are the results of studies of the activity of basal ganglia neurons in relation to behavior. Characterization of a unified theory of basal ganglia function is likely to come in the form of a single algorithm which is applied to cortical and thalamic input of different modalities. To elucidate this algorithm, behavioral correlates of the activity of basal ganglia neurons will have to be registered with the intricate framework of basal ganglia anatomy.

The striatum, or input stage of the basal ganglia, consists mostly of phasically firing neurons which project to other nuclei. It has been difficult to obtain electrophysiological recordings of large numbers of these neurons for analysis of properties of ensemble activity. The tetrode preparation of Matthew Wilson and Bruce McNaughton, which allows observation of the activity of large numbers of neurons organized in very local groups around each tetrode in awake, behaving rodents, seemingly has great potential for recording ensemble activity in relation to striatal subcompartments as well as to behavior. I helped to adapt this preparation for use in rodent striatal recordings in collaboration with Drs. Mandar Jog and Chris Connolly within the laboratory of Dr. Ann Graybiel. Section 3 describes the original preparation, followed by the modifications we introduced.

The first journal paper to result from this work was a study of how neuronal recruitment in dorsolateral rodent striatum in correlation with task events changes over the period of acquisition of a T-maze stimulus-response learning task (Jog et al., 1999). Its similarities and differences with other rodent studies of stimulus-response learning-related striatal neuronal activity inspire the proposal of a set of experiments to arrive at a consistent characterization of striatal neuronal activity in temporal relation to the acquisition of stimulus-response tasks, to localize task-responsive neurons relative to striatal subcompartments, and to observe, apparently for the first time, neuronal activity changes in basal ganglia output areas correlated with acquisition of stimulus-response tasks. Section 4 describes the background, aims, designs and methods for the proposed experiments. These studies are expected to benefit greatly from the superior ability of tetrodes to isolate separate sources of neuronal activity in local areas on the spatial scale of striatal substructures.

## 2 Striatal compartments and neuronal types

The basal ganglia (Figure 1) were once conceptualized as an “extrapyramidal” motor control system due to their implication in the motor abnormalities of Parkinson’s and Huntington’s diseases despite lacking direct connections to the spinal cord. In the last couple of decades, however, they have become associated with an array of disparate disorders and functions, including obsessive-compulsive disorder, Tourette’s syndrome, drug addiction, motor and nonmotor sequence learning, and motor and nonmotor habit formation. This diversity of involvement is not surprising, given that the basal ganglia (in primates) receive input from the

whole of cerebral cortex, except for primary visual and auditory areas (Mink, 1996), in turn projecting via thalamic nuclei to the cortical areas involved in motor and cognitive sequencing, decision-making, and action planning – the prefrontal, premotor, supplementary motor, and motor cortices. With such widespread afferent projections, a unified description of basal ganglia “function” is likely to be expressed in terms of a common transformation performed on input from different areas of cortex. Accordingly, anatomical and functional studies seek to define characteristics of that transformation.

Studies of the anatomical connections among the basal ganglia in primates and rodents have given rise to three major unifying paradigms. The basal ganglia are thought to be grossly segregated into five parallel circuits, defined by their eventual output areas in neocortex, which in turn influence activity in their input areas (Alexander and Crutcher, 1990). The “oculomotor” circuit projects to the frontal and supplemental eye fields; two “prefrontal” circuits project to dorsolateral prefrontal and lateral orbitofrontal cortex, respectively; the “limbic” circuit projects to anterior cingulate and medial orbitofrontal cortices; and the “motor” circuit projects to all precentral motor fields. Within each of these circuits (except perhaps for the limbic circuit), most researchers accept the definition of “direct” and “indirect” pathways (the latter projecting via the external globus pallidus and subthalamic nucleus) which are thought to act in opposition in order to limit or focus striatal input to basal ganglia output areas (but see (Parent et al., 2001)). Finally, researchers have debated the degree of convergence of cortical inputs through the stages of basal ganglia processing. Some convergence must occur, given the relative numbers of corticostriatal neurons, striatal neurons and basal ganglia output neurons: in each hemisphere, roughly 9 million to 3 million to 30,000 in rats (Oorschot, 1996; Zheng and Wilson, 2002). Yet some early tracing studies in primates seemed to indicate a great deal of parallelism in basal ganglia organization (Parent, 1990; Hazrati and Parent, 1992). Moreover, electrophysiological studies have demonstrated that GPi neurons are responsive to many of the same behavioral parameters as striatal units recorded in the same experiments (Nambu et al., 1990; Gardiner and Kitai, 1992; Kimura et al., 1996).

The prevailing conception is that convergence versus parallelism is a false dichotomy. Rather, inputs from cortex to basal ganglia diverge and converge in multiple ways to produce a large number of functionally specialized channels. Tracer injections into a single body part representation in SI label multiple zones in the sensorimotor striatum of primates, and projections from homologous body part representations within different areas of ipsilateral somatosensory and motor cortices tend to overlap in striatum, while projections from nonhomologous areas tend not to overlap (Flaherty and Graybiel, 1991, 1993b). Analogously, retrograde tracer injected into primate GPe and GPi labels patches in striatum (Flaherty and Graybiel, 1993a). Some of the patches labeled by anterograde tracers from cortex match patches labeled by retrograde tracers in striatum, indicating a reconvergence of cortical inputs in pallidum after some processing and combination with perhaps diverse sets of other information in divergent patches in striatum (Flaherty and Graybiel, 1994). Very interestingly, (Hoover et al., 2003) found via tracer injections into rodent SI cortex that corticostriatal projections from different components of the forelimb representation are more likely to terminate in overlapping regions of striatum than are projections from separate body parts (i.e., whiskers, hindpaw and forepaw). Thus, body parts which tend to move in coordination tend to have spatially grouped striatal representations.



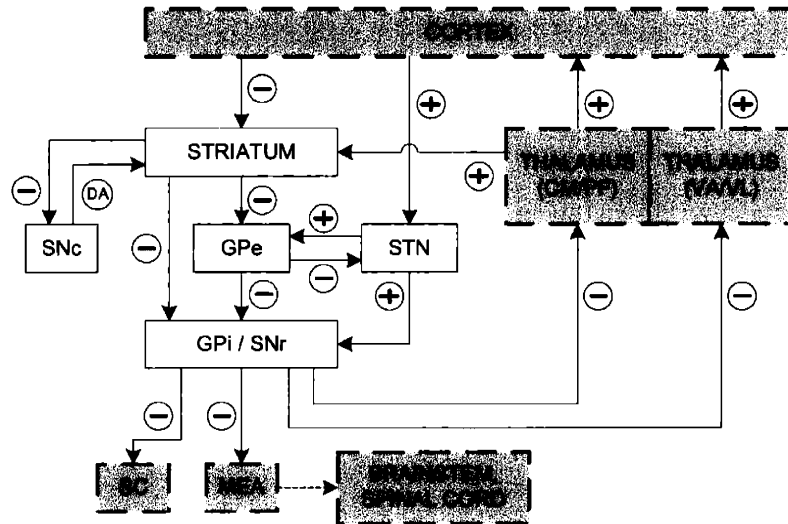


**Figure 1: Major connections of the basal ganglia. GPe= globus pallidus external segment; GPI = globus pallidus internal segment/entopeduncular nucleus (rodents); SNr = substantia nigra pars reticulata; SNc = substantia nigra pars compacta; STN = subthalamic nucleus; SC = superior colliculus; MEA= midbrain extrapyramidal area; CM/PF = centromedian and parafascicular thalamic nuclei; VA/VL = ventral anterior and ventrolateral thalamic nuclei; (+) = excitatory (glutamatergic) inputs; (-) = inhibitory (GABAergic + various peptides) inputs; (DA) = dopaminergic inputs.**

The modular organization of corticostriatal projections thus constructs a somatotopy in the striatal sector to which sensory and motor cortical areas project (dorsolateral striatum, in rodents). In rats, primates, and humans, various tracing, imaging, and neuronal recording methods show consistent within-species arrangements of striatal somatosensory and motor body part representations (Alexander and DeLong, 1985; Brown, 1992; Brown and Sharp, 1995; Cho and West, 1997; Brown et al., 1998; Maillard et al., 2000). (Liles and Updyke, 1985) both traced the projection from macaque primary motor cortex digit and wrist area to putamen and recorded from putamen neurons which responded to voluntary wrist movements, to verify that the somatotopy marked out by the corticostriatal projection corresponds to response properties of striatal neurons. In rats, the diameters of body part representations mapped by DG autoradiography (which images metabolic activity in the axon terminals of corticostriatal neurons) and extracellular recording from striatal neurons range from roughly 250-700 microns (Brown, 1992; Cho and West, 1997).

The systems of patches of striatal neurons with afferents from cortex and/or efferents to GPe, GPI, and SNr all fall into a “matrix” compartment which surrounds a set of interconnected modules termed “striosomes” which have limbic and some prefrontal afferents and possibly reciprocal projections to the dopaminergic SNc (Graybiel, 1990; Eblen and Graybiel, 1995). In rats, the cortical inputs to striosomes originate in the deep parts of layer 5, and matrix inputs originate from upper layer 5 and supragranular layers. However, it seems that neocortical areas in rat have few corticostriatal neurons in deep layer 5, meaning that striosomal inputs are predominantly from allocortical areas, and that therefore the functional distinctions between input areas of striosomes and matrix in rats are consistent with those in primates (Gerfen, 1992). Striosomes are distinguishable from matrix by a number of neurochemical markers, including AChE, calbindin, and mu-opioid receptors, which have species-specific and striatal region-

specific distributions (Groves et al., 1995). Rodent striosomes seem to be scaled similarly to modules in the matrix (“matrisomes”), i.e., they are a few hundred microns in diameter (Brown et al., 2002). Striosomes’ connection patterns suggest that their activity may influence dopaminergic levels in striatum, although apparently the matrix receives its dopaminergic inputs specifically from cell group A8, so that the DA regulation may be confined to striosomes themselves (Graybiel, 1990). (White and Hiroi, 1998) noted that rats were more likely, and more quick, to learn to press a bar to produce electrical self-stimulation if the stimulation electrode was placed in striosomes rather than matrix, suggesting that stimulation of striosomal neurons has a “rewarding” effect. (Brown et al., 2002), on the other hand, used DG autoradiographic mapping to image regions of high metabolic activity in the axon terminals of cortical projections to rodent striatum during walking, gentle restraint, and focal tactile stimulation under gentle restraint, and found that activity responsive to these presumably motivationally neutral behaviors was exclusive to projections to the matrix.

Striatal systems of organization are thus defined by neurochemistry and connections rather than cytoarchitectural distinctions. GABAergic medium-sized spiny projection neurons comprise, depending on the species, 75-96% of the neuronal population of striatum. These neurons have somata of 10-20 microns in diameter which emit several dendritic trunks that branch within 20 microns from soma into densely spiny branches (Kawaguchi et al., 1990). Depending on their compartmental location and target, MSNs contain combinations of dynorphin, enkephalin, and substance P (Mink, 1996). Most of the remaining neurons are large, aspiny cholinergic interneurons which are located in the matrix near striosomal borders, but some of whose dendrites may cross striosomal boundaries, perhaps facilitating sharing of information between compartments. Other known cell types are also medium-sized to large, aspiny GABAergic interneurons which are located in the matrix with dendrites crossing striosomal borders, containing somatostatin/ nitric oxide synthase /neuropeptide Y and parvalbumin (Kawaguchi et al., 1990; Kawaguchi, 1997).

MSNs have radiating dendritic fields of roughly 200-400 microns in diameter (Kawaguchi et al., 1990), meaning that a striosome or matrisome is about the size of 1-3 dendritic fields. Dendritic fields do not tend to cross striosomal/matrix borders. Most MSNs have axon collateral fields which ramify in the striatum with a diameter of roughly 400 microns and which overlap with their dendritic fields, suggesting a mechanism for recurrent inhibition. A smaller set of MSNs has local axon collateral fields with diameters of 1-2 mm, which extend to the dendritic fields of neighboring neurons and could provide a mechanism for collateral inhibition (Kawaguchi et al., 1990). In fact, (Tunstall et al., 2002), in recording from pairs of MSNs in slices of adult rat striatum, have described weak unidirectional GABA<sub>A</sub> receptor-mediated inhibitory interactions between MSNs. In target areas, axonal arborizations extend from 400 to 600 microns in diameter (Kawaguchi et al., 1990).

MSNs receive excitatory glutamatergic input from often bilateral corticostriatal projections, two-thirds of which terminate on the heads of dendritic spines (Groves et al., 1995). The corticostriatal axons have both focal arborizations, on the scale of striosomes and matrisomes, and extended arborizations, which could occupy as much as 14% of the total volume of rat striatum (Zheng and Wilson, 2002). There are also excitatory glutamatergic inputs from the centromedian and parafascicular thalamic nuclei, but these are less important in rats than in some other species (Groves et al., 1995). Cholinergic input comes from the large, aspiny interneurons, and GABAergic and peptidergic input from the other interneuron classes and nearby medium

spiny neurons. Dopaminergic input from SNc terminates primarily on shafts of the spines, with a single axon synapsing at several locations on a single dendrite as well as on multiple dendrites of multiple neurons (Groves et al., 1994). There is evidence for presynaptic interactions between glutamatergic (cortical) and dopaminergic (SNc) axon terminals which synapse onto nearby sites on the same MSN, which could modulate the strength of cortical synaptic inputs via temporal coincidence with reward-predicting signals from SNc (Groves et al., 1995). In general, extrinsic inputs to MSNs synapse on distal dendrites, while inputs from other striatal neurons synapse on proximal dendrites and the cell body (Parent, 1990).

Single MSNs are estimated to have roughly 5400 corticostriatal synapses (Kincaid et al., 1998). Within the area of a single dendritic field, a corticostriatal axon makes at maximum 250 en passant synaptic connections (Zheng and Wilson, 2002). However, there are roughly 2850 MSN somas within the volume of one dendritic field, so assuming one synapse per MSN, a maximum of 9% of neurons from that volume can receive input from a single corticostriatal axon (Zheng and Wilson, 2002). Therefore in general it is expected that the innervation of single MSNs by single corticostriatal neurons is very sparse. Moreover, the synaptic inputs are individually rather weak (Wilson, 1995). It is unknown how many corticostriatal synapses must be activated to fire an MSN, but this number has been estimated at 150 (Wilson, 1995). Thus, firing an MSN requires the coordinated activity of many corticostriatal neurons. The evoked corticostriatal EPSP has a duration of approximately 25 ms, so a large number of afferent neurons must fire within this time window (Wilson, 1995). MSNs have a bistable resting potential, with the lower value or “down” state around  $-80$  mV caused by a very powerful inwardly rectifying potassium current which shunts uncorrelated synaptic activations. It is believed that this current is distributed over the dendrites, which would mean that large numbers of synapses throughout the dendritic tree would have to be activated in coordination to depolarize the membrane enough to inactivate the rectifying current. The membrane potential then stabilizes around  $-50$  to  $-55$  mV, due to activation of a set of outwardly rectifying potassium currents. If a sufficient level of input is maintained in this “up” state, the neuron is then likely to fire action potentials; when the input level drops, the inward rectifying current will be activated and the membrane potential will once again stabilize in the “down” state (Wilson, 1995). These “up” and “down” states have been observed in slices and in urethane-anesthetized animals (Wickens and Wilson, 1998), and phasic firing patterns indicative of the operation of these states in awake animals have been observed in extracellular recording studies (Jog et al., 1996). (Wickens and Wilson, 1998) investigated in vivo a class of “silent” medium spiny neurons and found that their “up” states were slightly more hyperpolarized than those of firing neurons. The voltage dependences of the potassium conductances which determine “up” states are tunable by modulatory actions of, e.g., acetylcholine (Akins et al., 1990).

The cholinergic interneurons have soma of 20-50 microns in diameter, and smooth radiating dendrites which extend 0.5 – 1 mm in diameter, terminating in fine tufts (Kawaguchi, 1997; Bennett and Wilson, 1998). In rodents, the density of these neurons is highest in dorsolateral (sensorimotor) striatum (Kubota and Kawaguchi, 1993). Their morphology and electrophysiological properties match those of tonically active neurons (TANs) recorded from primates in vivo (Kawaguchi, 1993). Moreover, TANs, like cholinergic neurons, tend to be found in the matrix near the borders of striosomes (Kawaguchi et al., 1990; Aosaki et al., 1994). Inputs to TANs in rodents and primates come from cortex and the centromedian and parafascicular thalamic nuclei (Kawaguchi, 1997; Matsumoto et al., 2001). TANs fire spikes of half-amplitude width of at least 1 ms, at a rate of 3-10 Hz with a characteristic long

afterhyperpolarization (Kawaguchi, 1997; Bennett and Wilson, 1998). The spontaneous firing is due to intrinsic membrane properties which ensure that there is no resting potential (Bennett et al., 2000). Synaptic inputs regulate the timing of spikes: 1-5 mV AMPA receptor-mediated EPSPs produce a decrease in the ISI if they occur more than 0.4 ISI after the first spike, while GABA<sub>A</sub> receptor-mediated IPSPs prolong the ISI (Bennett and Wilson, 1998).

TANs in primates have been shown to acquire pause responses with 90-ms latency to visual or auditory cues over the course of classical conditioning (Aosaki et al., 1994; Aosaki et al., 1995). The effect seems to recruit TANs over large extents of striatum. Thalamic inputs from the centromedian and parafascicular nuclei have similar responses to stimuli, without respect to their association with reward. When these areas were temporarily inactivated with muscimol, the TAN pausing response was almost abolished, and behavioral responses to the conditioned stimuli were diminished (Matsumoto et al., 2001). TAN firing in relation to reward may be mediated by D1 inputs, which can enhance the afterhyperpolarization length (Bennett and Wilson, 1998). TANs may help to turn MSNs “on” or “off” by acetylcholine-mediated modulation of potassium conductances regulating the level of “up” states. Pauses to conditioned cues could change the level of ACh in targeted MSNs. The particular presence of TANs in sensorimotor striatum of rodents suggests an involvement in motor learning.

Parvalbumin-containing GABAergic interneurons receive input from cortex and have the shortest duration action potentials of all the identified striatal neuronal types: half-amplitude widths of less than 0.4 ms. They are called FS or “fast-spiking” interneurons due to high maximal sustained firing frequencies of roughly 200 Hz (Kawaguchi, 1993, 1997; Koos and Tepper, 1999). These neurons are connected by gap junctions (Kawaguchi et al., 1995). (Koos and Tepper, 1999) found that even single action potentials of one rodent FS neuron can significantly decrease the momentary firing rate of its MSN targets. They point out, additionally, that single FS interneurons may innervate over one hundred MSNs. The strong inhibitory connection between FS neurons and MSNs, along with the widespread projections to MSNs from single FS neurons and the electrotonic coupling between FS neurons, would seem to provide a method of simultaneously inhibiting large groups of MSNs which is much more effective than the weak MSN collateral inhibition found by (Tunstall et al., 2002).

Extracellular recordings of primate and rodent MSN activity in correlation to behavior have yielded responses to a wide range of phenomena, including: movement direction, target direction, and muscle pattern, firing shortly before or after movement initiation (Crutcher and Alexander, 1990; Kimura, 1990; Gardiner and Kitai, 1992); sequences and sequence learning (Kimura, 1990; Kermadi and Joseph, 1995); eye movement, visual stimuli, and movement set (Hikosaka et al., 1989); cues which signal movement initiation (Romo et al., 1992); instruction-induced movement preparation (Schultz and Romo, 1992); reward and reward expectation (Schultz et al., 1995); stimulus-response learning (Carelli et al., 1997; Jog et al., 1999). Given the diverse nature of cortical input to striatum, it is expected that a wide range of responses would be observed in single neurons. Any “coding” performed by striatum is thus likely to involve ensembles of neurons rather than single neurons, and most likely those ensembles which are already grouped together in striosomal and matrisomal modules. Thus an extracellular recording technique which could record multiple members of such local groups of neurons would be a valuable investigative method in striatum.

## **3 Adaptation of tetrodes for study of rodent striatum**

### **3.1 Technical needs of a striatal extracellular recording system**

An ideal system for recording extracellular spikes from the striatum would have the greatest possible capacity for accurately assigning spikes recorded at a single site to putative neuronal sources. Proper attribution to sources of spikes recorded at a single site allows investigation of the electrophysiological behavior of local groups of neurons at spatial scales comparable to the striatum's small-scale anatomical structures: striosomes, input or output matrixes, and/or body part areas.

The choice of recording technique depends upon to what extent the neurons of interest act as point sources of extracellularly recorded spikes. In such a case, the neuronal source emits an action potential with amplitude at the soma and waveshape constant over time and which propagates (in a medium with low or no dispersion) as a spherical wavefront centered on the source. However, in reality, action potentials from the same neuron often show variation in amplitude and waveshape over space as well as time. (Rall, 1962) points out that the dendrites of an active neuron affect its extracellular signal via the summation of passive backpropagating dendritic currents with the somatic action potential. Such dendritic effects cause the shape and amplitude of the extracellular signal to vary according to the direction of the electrode from the source. For example, passive currents conducted along the apical dendrite of a hippocampal CA1 pyramidal neuron add and subtract from the extracellular action potential so that in some directions it can be detected from hundreds of microns away (Henze et al., 2000). This summation becomes further complicated in neurons (e.g., some types of cortical interneurons) in which the site of action potential generation can vary unpredictably between various dendrites, thereby also propagating unevenly to other dendrites. As a result, the variability in amplitude of extracellular signals from such neurons can be as high as 80% (Nadasdy, 1998). Additionally, neocortical and hippocampal pyramidal neurons frequently emit bursts of action potentials in which the amplitude of later action potentials is significantly decreased relative to earlier ones, while the spike width is increased (Harris et al., 2000). Furthermore, (Fee et al., 1996b) and (Quirk and Wilson, 1999) report a similar amplitude and waveshape variability in nonbursting rat vibrissa and hippocampal pyramidal neurons, up to interspike intervals of 100 to 150 ms.

Single-electrode recording of multiple units is most effective when the signals may easily be separated according to differing waveshape, which occurs when the waveshape is a function of direction as described above, and/or when there are a mixture of neuronal types near the electrode. In this situation, simple waveshape parameters such as spike width, or more complex parameters like uncorrelated components of the waveform (principal components), may be defined and used to classify the signals. However, waveshape analyses become much less useful when the waveshapes of signals from a neuron vary depending on their interspike intervals. Moreover, often only one type of neuron is of interest, and if there is more than one of this type of source in a certain direction from the electrode, or if these neurons behave like point sources, waveshape analysis is fairly powerless. In this case, parameters related to the voltage (or power) of the signals, which vary inversely (or as the square of the inverse) with the distance of signal sources from the electrode, provide the only means of signal discrimination. Therefore, with a single electrode (in a uniformly dissipative medium), signals from sources of the same type

which are at an equal distance from the electrode but lie in different directions are not discriminable.

However, a recording electrode with four very closely-spaced non-coplanar tips, or “tetraode,” can be expected to be superior at correctly assigning spikes to sources on a spatial basis. In theory, under the point source assumption, the tetraode’s geometry enables the unique determination of all positions in three-dimensional space. With a single electrode tip, sources of the same type cannot be distinguished from each other if they lie on the same spherical surface centered on the tip (Figure 2a). Adding a second tip to the first allows every point in three-dimensional space to be expressed as lying on the intersection of two spheres centered around the two tips (Figure 2b). In general, the intersection of the two spheres is a circle; the two spheres intersect in a single point only for points along the line through the two tips. Therefore, sources not in line with the tips cannot be distinguished from each other if they lie on the same circular intersection of two spheres centered around the two tips. If a third tip is added, a sphere centered on this tip will intersect the circle defined by the intersection of the other two spheres (Figure 2c and Figure 2d). In general, this intersection will consist of two points on the circle which are at equal distances above and below the plane of the three electrode tips. In contrast, the two points at the top and the bottom of the circle lie in the plane of the three electrode tips, and are uniquely picked out by the intersection of the sphere with the circle. Thus, sources located at equal distances above and below the plane of the three electrode tips cannot be distinguished from each other. Finally, the addition of a fourth tip out of the plane of the other three distinguishes all points in three-dimensional space.

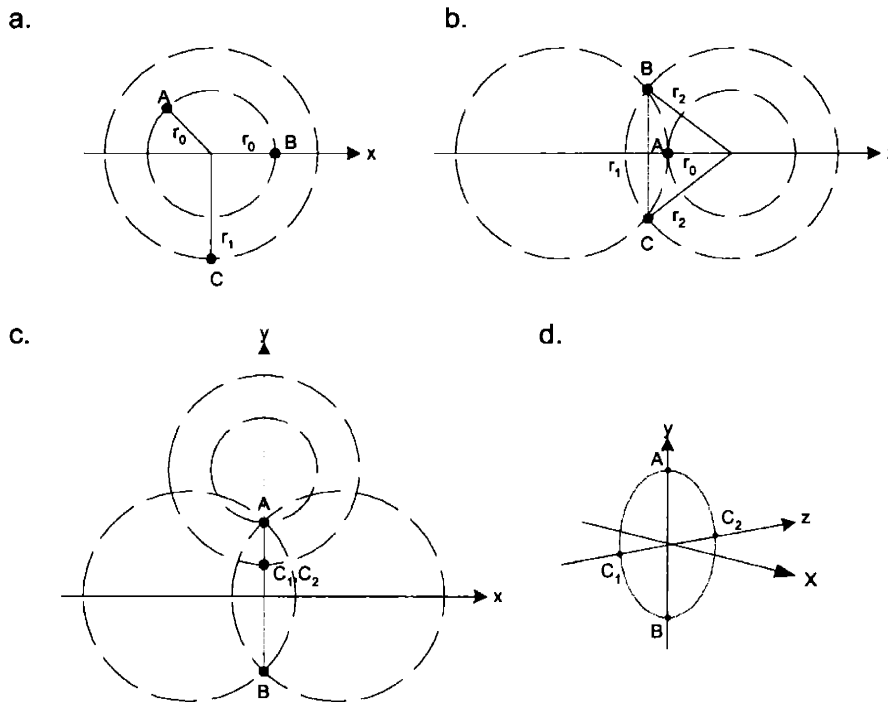


**Figure 2: The four tetraode tips uniquely identify points in 3D space. (a) One tip: points A and B cannot be distinguished. (b) Two tips: points B and C cannot be distinguished. (c-d) Three tips: points C1 and C2 cannot be distinguished.**

Even when the point source assumption does not hold, there is still a variation in the signal voltage with respect to distance from the source, and a variation in the waveshape with respect to direction from the source, so that relative differences in waveshape as well as voltage-related parameters across the four tetrode tips provide improved capacity to classify the extracellular signals. (Gray et al., 1995) demonstrated that the peak-to-peak amplitudes of extracellular signals on the four tetrode channels were more effective than amplitude or waveshape components on single electrodes or stereotrodes for classifying signals recorded from neurons in cat striate cortex. Not only were signals from different sources more easily distinguishable, but signals from the same source whose amplitudes and waveshapes varied with time were correctly classifiable. (Harris et al., 2000) recorded intracellularly and extracellularly from a group of hippocampal CA1 pyramidal neurons, producing a set of correctly labeled extracellular signals which they decomposed into principal components and used to train a neural network classifier in order to obtain estimates of the optimal classification power of a number of single electrodes and tetrodes. While error estimates differed greatly from wire to wire, the best single wires had roughly double the error rates of the tetrodes.

Given the assumption of neurons as point sources (and of low or no dispersion in the extracellular medium), tetrodes not only give the ability to uniquely *distinguish* sources at all positions in three-dimensional space, but also to *localize* them, given the appropriate calibration factors, which include the measured distances between the tetrode tips. If putative medium spiny neurons could be localized as well as identified by classification of their signals, the electrophysiological behavior of local groups of MSNs could potentially be registered with striosomes, input/output matrixes, or body part maps. The question is, does the point-source assumption basically hold in recording from medium spiny neurons?

According to, e.g., (Kawaguchi et al., 1990), medium spiny neurons have roughly radially symmetrical dendrites. Therefore, as viewed from any location outside the dendritic tree, passive currents in the dendrites will sum to zero, meaning that the dendritic currents will not alter the extracellular profile of the action potential (Rall, 1962). Secondly, the site of action potential generation should be stable within MSNs, as the generation of action potentials in these neurons depends upon the integration within the cell soma of postsynaptic potentials occurring concurrently in synapses all over the dendritic tree. Furthermore, medium spiny neurons are not observed to produce high-frequency bursts under normal conditions, although it is unknown whether amplitude and waveshape variability occur in non-bursting conditions. As a result, when signals from a medium spiny neuron are observed from outside its dendritic tree in an animal in normal health, the neuron is, to a good approximation, a point source. However, it is important to note that the dendritic tree of a medium spiny neuron has a diameter of roughly 200-400 microns (Kawaguchi et al., 1990; Plenz and Kitai, 1998). As tetrodes as used by (Wilson and McNaughton, 1993; Gray et al., 1995; Jog et al., 1999) have a diameter of approximately 50 microns, it is possible for a tetrode to be positioned within the dendritic tree of one or several neurons, in which case not all signals recorded by the tetrode can be considered to come from point sources.

For investigating the behavior of local groups of medium spiny neurons in striatum, we adapted the tetrode recording system developed by (Wilson and McNaughton, 1993) which uses multiple independently movable tetrodes in awake, freely-behaving rodents (Figure 3). The natural motor behavior allowed by this preparation seems obviously important for inquiry into basal ganglia electrophysiology. Several modifications were made in order to further augment

the system's potential for investigating striatum, including increasing the rigidity and integrity of tetrodes, developing an in vivo protocol for verifying tetrode positions, and calibrating tetrode tip geometry to reconstruct the positions of recorded sources. Additionally, we developed a reusable drive for holding and advancing the tetrodes, and novel software for visualizing, clustering, and analyzing the statistical properties of the neuronal data.

## 3.2 Wilson-McNaughton tetrode recording system

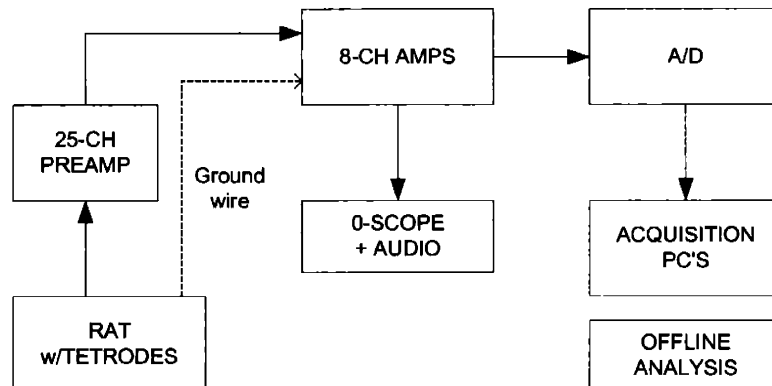


**Figure 3: Schematic of the Wilson-McNaughton tetrode preparation.**

### 3.2.1 *Manufacture and deployment of tetrodes*

The original Wilson-McNaughton apparatus has been previously described in, e.g., (Wilson and McNaughton, 1993; Gray et al., 1995), but will be reviewed here for clarity in the subsequent discussion of our modifications. Tetrodes are made by hand, from 12-micron diameter (including the polyimide insulation) nickel chromium wire (Kanthal, Nikrothal; formerly H.P. Reid, nichrome) which is doubled twice, suspended over a magnetic stirrer and twisted by attaching a magnetic weight to its end. The insulation on the outside of the twisted wires is partially melded together by brief application of a heat gun. The lower end is trimmed with scissors, and the upper end, which is a double loop, is cut into four tips, to each of which a small flame is briefly applied in order to remove the insulation there. The finished tetrode is about 10 cm long and 45 microns in diameter. After the tetrode is inserted into its microdrive (see below), its tips are plated with gold to increase the quality of signal transmission by suspending them in a gold cyanide solution and passing DC current through each tip; the plating is considered successful when the impedance as tested at 1 kHz is about 200-300 kohms.

Each tetrode is installed in a “microdrive” consisting of a series of telescoping stainless steel tubes in parallel with a set screw to allow advancement and retraction of the tetrode. A tetrode “drive” consists of several microdrives arranged in a rough circle around a central tube, bound together with dental acrylic. A central pole holds a connector with sufficient pins for the total number of tetrode channels in the drive, to which the upper tips are attached with conductive paint and shrink wrap.

When the drive is installed on an anesthetized rat (see section 4.3.4.3), several small stainless-steel bone screws are driven into (but not through!) the skull in order to provide support for the drive; at this point a wire is wrapped around one of the screws to serve as ground, and is



attached to a remaining pin on the connector. More dental acrylic is used to secure the drive to the screws, rendering it unretrievable upon sacrifice of the rat; a new drive is made for each animal.

### 3.2.2 Preamplifier stage

In recording, the drive is attached to a miniature preamplifier (Multichannel Concepts, model CFP-1020) with 25 channels, each with unity voltage gain, a high ( $>1000$  Mohm) input impedance, a low (500 ohm) output impedance, and a bandwidth of 0-1 MHz as measured at the -3 dB level. The preamplifier outputs run via an approximately 2-meter shielded cable to a bank of 8-channel programmable amplifiers (Neuralynx, Lynx-8), with a gain of 10,000 and an input resistance of 2.5 Mohms. Although the preamplifier does not improve the signal-to-noise ratio by direct amplification of the signal voltage, its presence solves two important problems in getting recorded signals to the amplifier. First, it maintains an upper frequency limit for the tetrode-amplifier circuit which is sufficient for accurately recording the waveforms of extracellular action potentials.

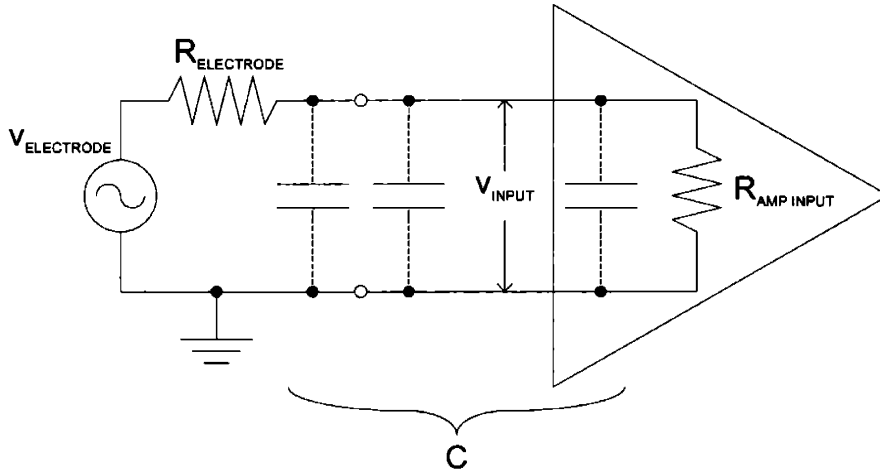


**Figure 4: Circuit between one tetrode channel and the amplifier.**

(Figure 4) diagrams the circuit between one tetrode channel and the amplifier as compared to ground, if there were no preamplifier. The input capacitance of the amplifier is in parallel with capacitances arising between the tetrode channel and ground (which may be lumped for convenience), and the resistances of the tetrode channel and amplifier input are also in parallel:

$$C = C_s + C_i \text{ and } R = \frac{R_s R_i}{R_s + R_i}$$

These quantities determine a time constant for the amplifier input circuit, which in turn determines its upper frequency limit:

$$\tau = RC \text{ and } f_{HIGH} = \frac{1}{2\pi\tau} = \frac{1}{2\pi RC}$$

Since the amplifier input resistance  $R_i$  is many orders of magnitude larger than the tetrode channel resistance  $R_s \approx 300$  kohms,  $R \approx R_s$ :

$$R = \frac{R_s R_i}{R_s + R_i} \approx \frac{(300 \times 10^3)(2.5 \times 10^6)}{(300 \times 10^3) + (2.5 \times 10^6)} = \frac{750 \times 10^9}{2.8 \times 10^6} \approx 270 \times 10^3 = 270 \text{ kohms}$$

$C$  for most regular wire gauges is on the order of 1 pF/cm (Kjartansson, personal communication).  $C_s$  is calculated using the length of the wire from the tip of the tetrode to the amplifier input, which is about 2 meters, so  $C \approx 200$  pF, and the upper frequency limit of the circuit is roughly given by:

$$f_{HIGH} \approx \frac{1}{2\pi(300 \times 10^3)(200 \times 10^{-12})} = \frac{1}{2\pi(9 \times 10^{-5})} \approx 0.03 \times 10^5 = 3 \text{ kHz}$$

This frequency limit is too low to accurately capture action potential waveforms. However, if the preamplifier is inserted into the circuit, the value of  $R_s$  becomes the output resistance of the preamplifier or 500 ohms, which is 600 times smaller than the resistance of the tetrode channel. Once again  $R$  is determined by  $R_s$ , which means that the upper frequency limit of the preamplifier-amplifier circuit is 600 times higher, or:

$$f_{HIGH} \approx \frac{1}{2\pi(500)(200 \times 10^{-12})} = \frac{1}{2\pi \times 10^{-7}} \approx 0.2 \times 10^7 = 2 \text{ MHz}$$

The maximum tolerable capacitance for the resulting tetrode-preamplifier circuit, assuming a generous upper frequency limit of 30 kHz, is equal to:

$$C_{MAX} = \frac{1}{2\pi R f_{HIGH}} \approx \frac{1}{2\pi(300 \times 10^3)(30 \times 10^3)} \approx .018 \times 10^{-9} = 18 \text{ pF}$$

Assuming the overestimate of  $C_s \approx 1$  pF/cm for the small diameter and short length of tetrode channels, and including the 4 pF input capacitance of the preamplifier, the maximum allowable tetrode length would be equal to:

$$C_s = C - C_i = 18 - 4 = 14 \text{ pF} + 1 \text{ pF/cm} = 14 \text{ cm}$$

which is in the range of the length which is used. True values for the upper frequency limit and maximum allowable tetrode length depend upon accurate values of probe resistance, cable length, and capacitances arising between all of the tetrode channels as well as from each channel to ground for both the tetrode wire and the 36-gauge wire used for each tetrode channel in the cable. However, it is clear that inclusion of these factors in our calculations will still result in limits which are more than sufficient for our purposes.

The preamplifier also minimizes noise arising from capacitive pickup of interference from surrounding electric fields, which is proportional to the total resistance of the circuit relative to ground (Kjartansson, personal communication). Without the preamplifier, this resistance would be approximately equal to  $R_s$ , the tetrode channel resistance of 300 kohms. With the preamplifier,  $R_s$  is roughly equal to the preamplifier output resistance, or 500 ohms, a reduction by a factor of about 600. Capacitive pickup is further reduced by surrounding the cable from the preamplifier to the amplifier with a grounded shield, and putting another grounded shield (a Faraday cage) from the rat's area to the ceiling.

### **3.2.3 Amplifier, A/D converter, and data acquisition stages**

The amplifiers' filter values on each channel are set to 0.6 and 9 kHz, defined at the -3 dB level. Limiting the bandwidth of the incoming neural signals allows their subsequent digitization at a sampling rate which balances the competing requirements for retention of important signal characteristics and minimization of storage space for the data. The lower filter value eliminates the DC component of the incoming signal, which is due to battery effects arising at the tetrode channel tip. The higher filter value of 9 kHz is chosen to include most of the spike's power and enough of its higher-frequency components to obtain reasonable estimates of the height and time of its peak. As the rise of the spike is the steepest part of the waveform, it contains most of the information about higher-frequency components; so some typical rise time of spikes from medium spiny neurons was determined by viewing the waveform with an analog oscilloscope, and its reciprocal was used to set the higher filter value. Alternatively, the higher filter value may be determined by sampling the spike waveform at a very high rate, performing a fast Fourier transform, and examining the resulting spike power spectrum to choose a frequency limit under which most of the power of the spike is contained.

By the sampling theorem, the minimum sampling rate for our bandwidth of about 9 kHz is 18 kHz. However, since the amplifier filters cannot be perfectly square (having in fact a falloff rate of 12 dB/octave), a slightly higher sampling rate is chosen to avoid aliasing of frequencies just outside the filter settings.

The amplified signals are sent through an analog-to-digital converter (Data Translation, model DT2821) and digitized at a sampling rate of 25 kHz per channel and buffered. Spikes are acquired from the data stream via the AD software package (M. Wilson, L. Frank) which, when the signal exceeds a user-defined threshold on any channel, stores with the appropriate time stamp 1.28 ms of data on all four channels of that tetrode. At a sampling rate of 25 kHz, this means that 32 data points are stored per spike per channel with a temporal resolution of 0.04 ms. The sample which reached threshold is set as the *n*th (probably fifth or sixth) sample, and the spike traces on the remaining three channels are registered accordingly.

### **3.2.4 Data analysis**

As described in (Gray et al., 1995), six two-dimensional projections of the data are displayed for each tetrode, showing all possible combinations of pairs of channels. Each data point consists of the peak-to-peak amplitude on two tetrode channels. Data points with similar values appear to cluster together, and are assumed to have the same neuronal source. The researcher draws boundaries around putative clusters, using the multiple projections to guide her judgment, and the resulting spike trains may be subsequently analyzed.

## **3.3 Modifications for use of tetrodes in striatum**

### **3.3.1 Tetrode manufacture**

Tetrodes manufactured as in section 3.2.1 sometimes went off-course as they were advanced toward striatum; to increase their strength, we dipped them (excluding the recording and connecting ends) into biocompatible cyanoacrylate glue (Pacer Technology), incidentally adding about 5 microns to the tetrode diameter. This step had the additional benefit of increasing the integrity of the tetrode geometry through penetration and advancement through brain tissue. (Jog

et al., 2002) report that microscopic examination of approximately 100 untreated tetrodes showed that their tips would splay apart by an average of 20-30 microns at least 70% of the time after cerebral penetration, increasing to 100% of the time after several days. Tetrodes treated with the glue, on the other hand, showed on average an over 90% reduction in tip splaying.

### 3.3.2 Drive manufacture

Handmade tetrode drives were time-consuming and relatively fragile. Moreover, in studying a motor-related area such as striatum, it is particularly important not to put an unnatural load on the animal. In collaboration with engineer Ray Harlan, we developed a reusable, autoclavable 6-12 tetrode drive machined from Delrin, with plastic set screws and polyimide rather than stainless steel telescoping tubes (inner diameters of 0.0159, 0.0062, and 0.0035 inches). The only remaining metal components were brass support rods for the set screws (Figure 5). These modifications decreased the weight of the drive from roughly 13 grams to 7 grams (Jog et al., 2002). Substitution of polyimide for steel tubes risked increasing the capacitance of the input-preamplifier circuit (see section 3.2.2), but in practice doesn't appear to have made a difference. To protect the drive from damage and dirt once installed on the animal, we developed a Lexan cone with a screwed-on cap which had holes to allow access to the tetrode set screws. The cone was shatterproof, lightweight, and heat resistant, with the removable cap allowing in situ repairs to drive components.



**Figure 5:** Reusable, autoclavable tetrode drive with Lexan cone. Reprinted from (Jog et al., 1997).

### 3.3.3 In-vivo tetrode localization by MRI

A rat implanted with a tetrode drive may be recorded from over the course of a month or two, during which period individual tetrodes may be advanced or retracted many times. Under these conditions, it seemed useful to develop a method for confirming the dorsoventral level of tetrodes at each stage of advancement, information which was unretrievable from histological analysis or from the firing characteristics of recorded sources. We worked with Dr. Leo Garrido of the Charlestown MRI facility of Massachusetts General Hospital to develop an MRI protocol for in vivo localization of tetrodes. Our redesigned drive, constructed from non-magnetic materials, is MRI-compatible, and brass bone screws are used instead of steel.

The Nikrothal alloy used for tetrodes is nonmagnetic or at most only weakly paramagnetic (Nikrothal spec sheet). Water (an approximation to extracellular fluid), on the other hand, is slightly diamagnetic, with a magnetic susceptibility of about  $-10^{-10}$ . This difference in magnetic

behavior leads to a signal loss in the region surrounding a tetrode, in practice producing a 180-micron wide artifact in a T1-weighted image as determined by imaging a tetrode in a water-filled Plexiglas cylinder. This is an adequate resolution for measuring dorsoventral positions of tetrodes, as well as confirming penetration to the rat striatum, which is roughly 3 mm in depth at our stereotaxic coordinates of entry, AP = +0.5 and ML = +3.7 mm relative to bregma (Thompson, 1978).

The imaging procedure takes about 40 minutes, and is described in (Jog et al., 2002). Images are acquired in a 2.0 T MRI system (Varian Associates, Palo Alto, CA) using a 2-D spin echo sequence with phase encoding. Inductively-coupled transmitter and receiver coils are placed on the head of the rat around the bottom of the cone surrounding the tetrode drive. The receiver bandwidth is 10 kHz. For all images, the field of view is 3.5 mm x 3.5 mm, with a resolution of 256 x 128 pixels and a slice thickness of 900 microns, i.e. a voxel size of 200 x 400 x 900 microns.

1. The rat is anesthetized and immobilized in a Plexiglas stereotaxic frame. (Intraperitoneal injection of 0.5 ml of 25% ketamine and 2.5% xylazine, both 100 mg/ml in 0.9% saline.)
2. A set of 7 proton-density-weighted coronal slices (TR = 1400 ms, TE = 20 ms) is acquired in order to find the A-P plane of the ends of the tetrodes, and to estimate their depth. For these slices, only two signals are acquired per phase encoding step.
3. A set of 3 or 4 T1-weighted horizontal slices (TR = 500 ms, TE = 20 ms) is acquired to pinpoint the depth of the tetrodes more precisely. For these slices, sixteen signals are acquired per phase encoding step.
4. While the proton density and T1-weighted images prove to have relatively small tetrode artifacts, they do not show much contrast between gray and white matter. It was found that T2-weighted images (TR = 800 ms, TE = 80 ms) show an enhanced differentiation of gray and white matter, but have a larger signal loss around the tetrodes due to the increased echo time (possibly due to inefficient spin energy transfer from brain tissue to the tetrode material). As needed, T2-weighted images are collected for superimposition with the T1-weighted images.

Tetrodes in the resulting images are identified by comparison with estimates of tetrode depths derived from records of the number of turns of their (0-80) set screws.

### ***3.3.4 Data visualization and clustering***

#### ***3.3.4.1 Elimination of EMG noise and non-MSN spikes***

As our interest is (currently) restricted to medium spiny neuron activity, action potentials from other neuronal types must be removed from the dataset (along with any EMG noise which triggered acquisition). Assuming that there is isotropic Gaussian variability of waveshapes across different signal source types, MSN signals may be separated from TAN signals and EMG

noise via minimum-Euclidean-distance classification. The distance from a normalized template  $\mathbf{N}$  to a waveform  $\mathbf{W}$ , both of which are 32-component vectors, may be expressed as follows:

$$\begin{aligned}\|\mathbf{W} - \mathbf{N}\|^2 &= (\mathbf{W} - \mathbf{N})^T (\mathbf{W} - \mathbf{N}) \\ &= -2\mathbf{N}^T \mathbf{W} + \mathbf{N}^T \mathbf{N} + \mathbf{W}^T \mathbf{W}\end{aligned}$$

Therefore, to find the *normalized*  $\mathbf{N}$  which is the minimum distance from a particular  $\mathbf{W}$ , it is sufficient to find the  $\mathbf{N}$  which maximizes the inner product of  $\mathbf{N}$  and  $\mathbf{W}$ .

Normalized templates for MSN signals, TAN signals, and EMG noise were created by averaging about 30 selected normalized examples of each waveform type. The inner product of each waveform  $\mathbf{W}_i$  on a channel  $n$ ,  $\mathbf{W}_{in}$ , is computed with each template  $\mathbf{N}_j$

$$b_{in} = \sum_{s=1}^{32} W_{in}(t_s) N_j(t_s)$$

These (positive) per-channel inner products are summed to produce a score,  $B_{ij}$ , for each template, and  $\mathbf{W}_i$  is classified according to the template with the highest score:

$$B_{ij} = \sum_{n=0, b_{in} > 0}^3 b_{in}$$

#### 3.3.4.2 Generation of power measures for clustering

(Gray et al., 1995) found that clustering spikes according to their peak-to-peak voltages at the tetrode tips provided optimal separation of spikes originating from different neuronal sources of the same type, even when the waveforms from a single source vary with respect to time. However, measurement of peak-to-peak voltage is sensitive to whether the peak is sampled as well as to any fluctuations in noise around the peak which do not affect the signal at all four tetrode tips. On the other hand, the average power, which is calculated using the whole spike waveform, should be less sensitive to these considerations, perhaps providing even better separation of clusters.

If  $\mathbf{W}_n$ , the spike waveform on a channel  $n$  in units of microvolts, were a clean instance of an MSN action potential, its average power could be found by computing its autocorrelation:

$$R(\tau) = \frac{1}{T} \sum_{s=1}^{32} W_n(t_s) [W_n(t_s - \tau)] \text{ where values of } \tau \text{ are restricted to sample points.}$$

At  $\tau=0$ , when the two waveforms  $\mathbf{W}_n$  overlap perfectly, the autocorrelation peaks and is equal to the average power of the spike:

$$R(0) = \frac{1}{T} \sum_{s=1}^{32} [W_n(t_s)]^2$$

Since, however,  $\mathbf{W}_n$  probably contains some random noise, it would be better to eliminate that noise before calculating the average power of the waveform. Imagine cross-correlating  $\mathbf{W}_n$  with an idealized waveform of the same amplitude  $\mathbf{M}$ :

$$R(\tau) = \frac{1}{T} \sum_{s=1}^{32} W_n(t_s) [M(t_s - \tau)] \text{ where values of } \tau \text{ are restricted to sample points.}$$

This operation is very much like the autocorrelation above, except that the idealized waveform  $\mathbf{M}$  smoothes  $\mathbf{W}_n$ , averaging out uncorrelated noise. Thus the peak cross-correlation provides a cleaned-up figure for the average power of the spike.

Although a template of equal amplitude cannot be provided for every incoming  $\mathbf{W}_n$ , the normalized medium spiny template  $\mathbf{N}$ , which was initially used to extract medium spiny waveforms from the dataset, may be used to calculate a value  $S_n$  which is proportional to the average power of  $\mathbf{W}_n$ . In practice, the power measure  $S_n$  for  $\mathbf{W}_n$  is found by taking the derivative of the cross-correlation and searching for the first positive peak which is not near either of the edges of the window, and which can be matched with peaks at approximately the same time lag on the other three channels of the tetrode. The four power measures are stored with a timestamp equal to the original event timestamp plus the mean correlation lag.

Any noise events (usually generated by a strong external source) which escaped the initial cleansing of the dataset via template-matching will have roughly identical power measures on all four channels, and may be eliminated at this stage.

#### 3.3.4.3 Three-dimensional display of power measures

The resulting power measures were originally displayed in a three-dimensional rotatable plot in which each data point consisted of the power measures on three channels relative to the power on the fourth. Although intended as an improvement to comparing six static two-dimensional visualizations in order to identify clusters, this display still did not allow the use of all four power dimensions to distinguish clusters which were conflated in three-dimensional views. A later version of the software, as described in (Jog et al., 2002), was improved to include two side-by-side rotatable three-dimensional plots, with axes as the power on tetrode channels (0, 1, 2) and (1, 2, 3) respectively. A different color is assigned to each identified cluster in the display (Figure 6).

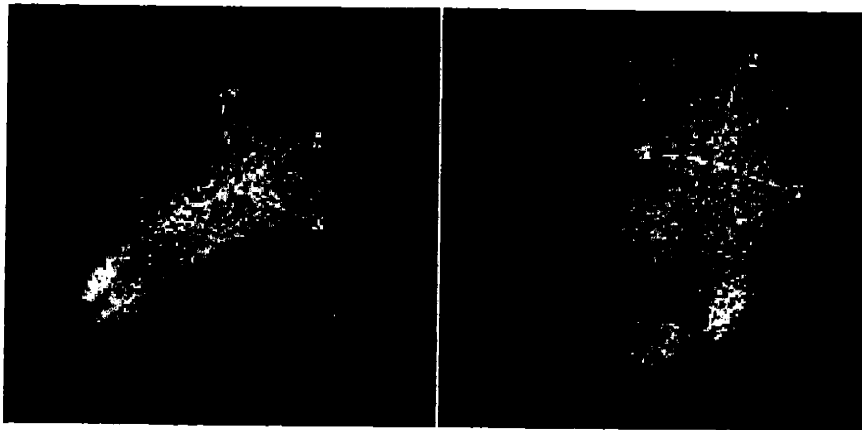


**Figure 6: 3-D cluster plot shown in two different rotations. Axes are the power measures on three tetrode channels. Reprinted from (Jog et al., 1998).**

#### 3.3.4.4 Automated clustering by K-means

Manual cluster cutting has the advantage that no assumptions need be made regarding the shapes or distributions of clusters. However, overlapping spikes will not be detected unless they happen to cluster together. Moreover, cluster boundaries tend to be unclear in the two- or three-dimensional spaces usable by human operators, causing the results to be subject to operator bias. Automatic clustering methods, on the other hand, can cluster in higher dimensions (in this case, four) based upon explicit criteria.

The K-means algorithm (Bishop, 1995) requires a human operator to select a number  $k$  of putative cluster centroids, and then partitions the dataset into disjoint clusters by minimizing some error measure related to the distances of points from cluster centroids over many iterations. We implemented the batch version of K-means, in which cluster centroids are only recomputed after all data points have been assigned to clusters. Typically, we choose a value for  $k$  which slightly overestimates the number of clusters we can see in the data ((Jog et al., 2002) report a typical value of  $k=12$ ) in order to allow the algorithm to separate any visually indistinct clusters and to capture outlying points into extra clusters. (Any overclustered data can be recombined later on the basis of post-hoc tests; see next section.) Additionally, we used to assign locations to our initial cluster centroids in order to optimize the solution, because the outcome of the K-means algorithm is sensitive to the initial conditions; e.g., a centroid which is too far away from any data points may never be updated. However, (Jog et al., 2002) report that the initial cluster centroids are randomly assigned in current versions of the software, which may necessitate more extensive post-hoc evaluation of the clustering solutions.

The classical choice of error measure for K-means is the sum of cluster variances:

$$E = \sum_{i=1}^k \sum_{\mathbf{S} \in p_i} \|\mathbf{S} - \boldsymbol{\mu}_i\|^2$$

where  $\boldsymbol{\mu}_i$  and  $p_i$  are the centroid and the set of four-dimensional power measures  $\mathbf{S}$  in cluster  $i$ . Use of this criterion, which is identical to the sum of squared Euclidean distances from cluster means, assumes an isotropic Gaussian distribution for points within clusters. The resulting spherical cluster boundaries poorly fit our data, which cluster ellipsoidally in three-dimensional projections (Figure 6). For visually distinct clusters, histograms of distances of cluster members from the cluster mean show a nearly Gaussian distribution (Jog et al., 1998). (Fee et al., 1996b) and (Harris et al., 2000) likewise found (for nonbursting rat vibrissal and hippocampal CA1 pyramidal cells, respectively) anisotropic, almost Gaussian distributions for points within their clusters, and furthermore that the power spectra of the background activity and differences of spike amplitudes from the cluster mean are roughly identical, indicating that cluster shape for nonbursting cells primarily results from background activity of neurons and axons of passage. (Fee et al., 1996b) additionally found that the background activity in rat vibrissal cortex could not be modeled as a stationary random Gaussian process, a result that probably generalizes to most brain areas; therefore, the nearly Gaussian distributions of clusters are likely a manifestation of the central limit theorem. (Overlapping spikes, waveshape variation in the absence of bursts, and electrode drift may be additional determinants of cluster shape.)

If it is assumed that clusters have anisotropic Gaussian distributions, the error measure needs to include cluster covariance. The Mahalanobis metric, unlike the Euclidean metric, weights



differences from a cluster mean by the cluster covariance matrix  $\bar{C}$ , effectively compressing distances along the axes of a cluster's elongation:

$$\|S - \mu_i\|_{MAHA}^2 = [S - \mu_i]^T \bar{C}^{-1} [S - \mu_i]$$

Replacing squared Euclidean distance in the error measure with squared Mahalanobis distance means that every time the cluster means are recomputed during a run of the K-means algorithm, the 4x4 covariance matrices describing the shape of each cluster must also be updated.

#### 3.3.4.5 *Post-hoc testing and adjustments*

Any manual or automatic clustering method must make decisions about low-power data points, outliers, and hard-to-classify areas between two or more indistinctly separated clusters, requiring post-hoc verification of the clustering results. To test each cluster for inclusion of false positives, we can make within-cluster interspike interval histograms for intervals up to 30 ms in either direction. Assuming a generous 5 ms refractory period for medium spiny neurons (although (Plenz and Kitai, 1998) report an AHP of  $8.6 \pm 1.3$  ms for cultured MSNs from Sprague-Dawley rats), we accept clusters in which 90% or more of the data points have interspike intervals above this threshold. Additionally, we can make plots which superimpose the per-channel waveforms of all data points within a cluster in order to assess the degree of presence of noise or noise-contaminated waveforms. Clusters with noisy-looking superimpositions (usually clusters of low-power data points, commingled with other clusters near the origin of the power space) are excluded from further analysis. Finally, pairs of identified clusters which are not visually well-separated may be recombined on the basis of comparing the refractory periods in their individual ISI histograms with their inter-cluster ISI histogram. The phasic, low frequency firing of MSNs means that refractory period tests should be interpreted with caution.

If many clusters in a dataset do not pass the false-positives test, the K-means procedure should probably be re-run with different choices for the number and/or location of initial means. If only some of the clusters do not pass one test or the other, it may be possible to improve them by removing outlying points. The user can delete points by hand, or exclude points beyond a specified Mahalanobis distance from the center of the cluster. (Since the Mahalanobis distance to a point is the Euclidean distance scaled by the variability of the cluster in the relevant direction, this method is equivalent to setting the cluster boundary at a multiple of the variance.)

#### 3.3.4.6 *Clustering by K-means versus human operators*

A recent paper by (Harris et al., 2000) compared the results of clustering by human operators with clustering by an unsupervised learning algorithm followed by post-hoc verification. Simultaneous intracellular and extracellular recordings were made from a group of hippocampal CA1 pyramidal neurons to obtain labeled extracellular data, which were used to train a two-layer neural network in order to obtain an estimate of the optimal error rate achievable for the data set by any clustering method (by minimizing a sum of two types of errors: false positives and false negatives). In relation to this ground truth, clustering by human operators with varying degrees of experience had "significantly greater" error, whereas the semi-automatic method produced error rates lower than any of the human operators and comparable to the optimum estimate of error. The clustering algorithm used was AutoClass (<http://ic.arc.nasa.gov/ic/projects/bayes->

group/autoclass/), a Bayesian learning algorithm which, unlike K-means, does not require the user to specify the number of classes present in the data. It would be interesting to similarly quantify the improvement in accuracy that we believe we obtain from using K-means instead of human operators.

#### *3.3.4.7 Clustering by power measures versus peak-to-peak voltage*

Accurate identification of clusters is obviously simpler when the clusters are better separated to begin with; (Jog et al., 2002) report that using power measures rather than peak-to-peak voltage (e.g., Wilson and McNaughton, 1993) results in clusters which, 74% of the time, are on average 8% more compact relative to the entire dataset. (Cluster compactness was determined by taking the ratio of the determinant of the cluster's covariance matrix and the determinant of the dataset's covariance matrix.) This result seems to support the suggestion that the separation of clusters may be improved by using a measure resembling average power.

#### *3.3.5 Reconstruction of source locations*

If medium spiny neurons closely approximate point sources, the direction as well as the distance of neurons from the tetrode may be recovered (see Figure 1), and in conjunction with measurements of the tetrode depth in the striatum derived from MRI (see section 3.3.3) may be used to reconstruct the locations of local groups of neurons recorded by all tetrodes over the recording lifetime of a rat. To the degree that such reconstructions are accurate, they may give a picture of neuronal activity on the spatial scale of striatal anatomical substructures such as striosomes or input/output matrixes, which in turn could be correlated with behavioral events.

To make spatial reconstruction possible, it is necessary to determine the relative positions of the tetrode channel tips and to assume that extracellular space is non-dissipative over the distances between sources and the tetrode and over the time of data collection. Any existing attenuation, even if uniform in all directions, would cause the spatial reconstruction procedure to overestimate distances of sources from the tetrode.

Calibration of relative channel tip positions is obtained in the process of gold-plating the tips (see section 3.2.1). As each channel of a tetrode is plated, it is labeled with a number (0,1,2, or 3) and its tip is identified under a microscope (BIOCOM, with attached digital camera). After all channels are plated, the tetrode is placed under the microscope again, and the inter-channel distances are measured in the x-y plane by counting pixels and in the z-plane by the calibration on the focus dial. (Both the pixel size and focus dial calibration are convertible by known factors to microns.) Three measurements of each distance are averaged to produce a mean figure with uncertainties.

##### *3.3.5.1 Determination of source position*

In the calculation of source positions, each source's average power as recorded from the tetrode tips is represented by its cluster centroid as determined by the K-means procedure. Given the preceding assumptions, the signal has a spherical wavefront described by the inverse-square law, and  $S$  for a particular tetrode tip  $n$  is proportional to the intensity  $I$  of the wavefront at the tetrode tip by a constant  $a$ , which reflects the effective tip cross-sectional area as well as the mismatch between the tetrode and preamplifier input resistances:

$$S_n = aI_n = \frac{aP}{4\pi r^2}$$

where  $r$  is the distance between the source and tetrode tip  $n$ , and  $P$  is the actual power output of the action potential. Solving for  $r^2$  and defining the quantity  $c$  as:

$$c = \frac{aP}{4\pi}$$

the inverse-square law becomes:

$$r^2 = \frac{c}{S_n} = x^2 + y^2 + z^2$$

Setting the origin of the coordinate system at the tip of channel 0, a system of four equations, representing four intersecting spheres centered around the tetrode tips, may be written to solve for the four unknowns:  $x, y, z$ , and  $c$ .

$$\frac{c}{S_0} = x^2 + y^2 + z^2$$

$$\frac{c}{S_1} = (x - x_1)^2 + (y - y_1)^2 + (z - z_1)^2$$

$$\frac{c}{S_2} = (x - x_2)^2 + (y - y_2)^2 + (z - z_2)^2$$

$$\frac{c}{S_3} = (x - x_3)^2 + (y - y_3)^2 + (z - z_3)^2$$

Subtracting the latter three equations from the first one and defining  $\Delta_n = x_n^2 + y_n^2 + z_n^2$  yields:

$$c\left(\frac{1}{S_0} - \frac{1}{S_1}\right) = 2xx_1 + 2yy_1 + 2zz_1 - \Delta_1$$

$$c\left(\frac{1}{S_0} - \frac{1}{S_2}\right) = 2xx_2 + 2yy_2 + 2zz_2 - \Delta_2$$

$$c\left(\frac{1}{S_0} - \frac{1}{S_3}\right) = 2xx_3 + 2yy_3 + 2zz_3 - \Delta_3$$

This system may be rewritten as follows:

$$c\mathbf{p} = 2\bar{\mathbf{A}}\mathbf{r} - \Delta, \text{ where } \mathbf{p} = \begin{bmatrix} \frac{1}{S_0} & \frac{1}{S_1} \\ \frac{1}{S_0} & \frac{1}{S_2} \\ \frac{1}{S_0} & \frac{1}{S_3} \end{bmatrix}, \bar{\mathbf{A}} = \begin{bmatrix} x_1 & y_1 & z_1 \\ x_2 & y_2 & z_2 \\ x_3 & y_3 & z_3 \end{bmatrix}, \mathbf{r} = \begin{bmatrix} x \\ y \\ z \end{bmatrix}, \text{ and } \Delta = \begin{bmatrix} \Delta_1 \\ \Delta_2 \\ \Delta_3 \end{bmatrix}.$$

$\bar{\mathbf{A}}$ , the matrix of the coordinates of tetrode tips 1-3 relative to tip 0, is invertible since the four tips are not coplanar (Figure 2), allowing us to solve for  $\mathbf{r}$  which has components  $x, y, z$ :

$$\mathbf{r} = \frac{c\bar{\mathbf{A}}^{-1}\mathbf{p} + \bar{\mathbf{A}}^{-1}\Delta}{2}$$

This solution vector is parameterized by the unknown  $c$ , which is related to the magnitude of  $\mathbf{r}$  as follows:

$$\frac{c}{S_0} = |\mathbf{r}|^2$$

Substituting  $\mathbf{r}$  into the above equation and solving for  $c$ , we arrive at a quadratic equation of the form:

$$\theta c^2 + 2(\phi - \frac{2}{S_0})c + \gamma = 0, \text{ where } \theta > 0 \text{ and } \gamma > 0. \text{ (see Appendix for details)}$$

There will thus usually be two real solutions for  $c$ , both either positive or negative; the solution with the greater absolute value is chosen, as the smaller one is generally too close to the tetrode tips (Jog et al., 1998). (Figure 7) illustrates the geometry of the solution.

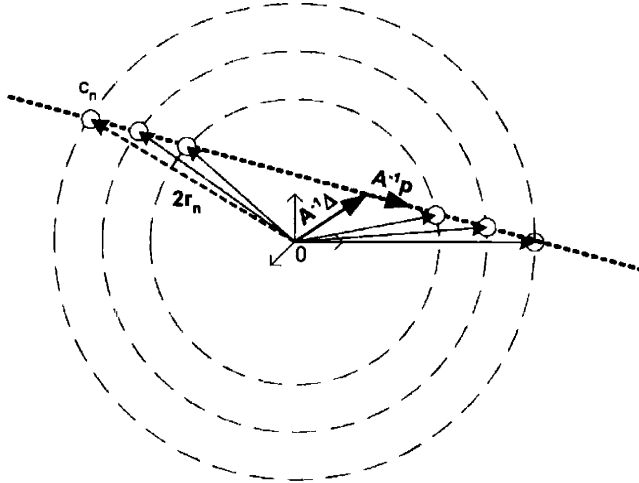


**Figure 7: Reconstruction of source position. The solution vector  $\mathbf{r}$  is parameterized by  $c$ .**

(Jog et al., 2002) report that reconstructions of source locations show that active cells on a tetrode are typically separated by distances of 20-50 microns, several times either the short ( $9 \pm 1$  microns) or long ( $12 \pm 1$  microns) somatic diameters of cultured Sprague-Dawley rat MSNs

reported by (Plenz and Kitai, 1998). The most distal sources with resolvable clusters are estimated to lie between 80 and 100 microns from the tetrode, a slightly larger figure than those empirically obtained by (Gray et al., 1995) and (Henze et al., 2000) of 65 and 50 microns, respectively. At least some of the discrepancy is likely due to the fact that we ignore dissipative properties of the extracellular medium in our calculations. However, assuming that the extracellular medium is homogeneous and isotropic, our spatial reconstructions of the *directions* of sources relative to the tetrode should remain useful.

### 3.4 Experimental results

With our tetrode preparation, (Jog et al., 1999), (Kubota et al., 2000) and (Hu et al., 2001) have demonstrated that the recruitment of single units in rat and mouse striatum apparently shifts its correlation with various phases of a T-maze procedural learning task as a function of learning, overtraining, extinction, and relearning. (See section 4.1 for further discussion.) Neuronal activity related to task acquisition should be further characterized with analysis of how statistical interactions between the firing patterns of multiple neurons appear and are modified over the course of task learning. For example, (Jog et al., 1997) examined the activity of roughly 20 units over the course of random walking or delayed alternation on a T-maze and found that the proportion of pairs of units showing 10-ms latency positive peaks in their pairwise interspike interval histograms increased from 15% prior to training to 40% after a week of T-maze training. Moreover, peaks in post-training pairwise ISI histograms were narrower than in pairwise ISI histograms of activity prior to training. This directional relationship of firing is unlikely to be caused by direct connection between MSNs; it is more likely that cortical afferents to these neurons are firing in this temporal relationship, which becomes tighter by the end of training.

In preliminary examination of data acquired from freely roaming Sprague-Dawley rats, initially reported in (Jog et al., 1996), we noted several features of the spontaneous ensemble activity for further investigation. First, there were periods in which the activity of several or all sources recorded on one tetrode would pause for up to a few hundred milliseconds. Secondly, the activity periods of some units located on different tetrodes appeared grossly coincident or reciprocal. Thirdly, sometimes most or all units recorded on one tetrode would fire one or a few spikes within a time period of 100-200 ms, surrounded by silent periods of roughly 200 ms. This activity pattern appeared as a “threadlike” structure on raster plots. Finally, several pairs of sources displayed a directional bias in their firing pattern, as shown by the presence or extent of peaks at 10-30 ms in their pairwise interspike interval histograms. While some of these observed features are suggestive (e.g., a pause across a group of nearby units could indicate some commonality of cortical inputs to those units), they must be definable so as to allow automated extraction from the data and testing for significance of frequency of occurrence before any correlation may be made with behavior or with activity in other regions of the striatum or cortex.

Construction of pairwise ISI histograms from MSN activity (as well as construction of JPSTH’s) is a tricky proposition, as the phasic firing patterns may violate the stationarity requirement at certain time regimes, and in general there is a paucity of spikes, which could cause artifacts. The individual ISI plots could be smoothed before or after computing the pairwise histogram, as in (Djurfeldt et al., 2001), who computed pairwise ISI histograms from the data of (Jog et al., 1999), bandpass filtered them to smooth out artifacts, and found peaks with widths of roughly 5 milliseconds and offsets of tens of milliseconds, in agreement with earlier results.

## 3.5 Suggestions for further work

### 3.5.1 *Mass production of tetrodes*

Each handmade wire tetrode has a different configuration of tips, with (Jog et al., 2002) reporting center-to-center tip separations averaging 20-30 microns in the x and y directions and 5-6 microns in the z direction. In practice, background activity limits detection of differences in voltage/power recorded across the tetrode tips, so that the maximum resolving distance of a tetrode depends upon the inter-tip distances. Therefore, the smaller separation in the z-dimension of our wire tetrodes could hamper separation of data from some of the recorded sources. Moreover, uncertainty in tip separations due to measurement errors or to subsequent alteration as the tetrode is advanced through brain tissue affects the accuracy of spatial reconstruction of sources. Both of these issues could be addressed by designing a silicon tetrode consisting of a single shank with recording sites which are separated in all three dimensions. Use of mass-produced silicon tetrodes would also save time and increase the probability that all tetrodes in a given drive are operational.

(Nadasdy, 1998) uses a silicon tetrode with four equally spaced recording sites in a linear configuration to separate signals based upon spatially-related parameters. The linear configuration of the channels permits the definition of two quantities for each neuronal signal: center of field, which is a weighted average of the four amplitudes measured at the channels, and interpolated field position, which uses cubic-spline interpolation of the amplitudes measured at the channels to estimate the location of peak amplitude along the line of the tetrode sites. The data is then plotted in a three dimensional space whose third coordinate is the sum or non-weighted average of the amplitudes across the four channels, and clustered using a K-means procedure.

### 3.5.2 *Additional clustering parameters*

Any signals in our dataset originating from neurons whose dendritic trees surround the tetrode do not satisfy the point source assumption, and can be expected to show some dependence of waveshape upon the location of their sources relative to the tetrode. Waveshape thus might be a useful additional parameter in clustering signals from MSNs, assuming that source locations are relatively stable over the length of a recording session and that waveshapes from a source do not vary with interspike intervals.

### 3.5.3 *Clustering algorithm*

#### 3.5.3.1 *K-means caveats*

Although we can run post-hoc tests on clusters generated by K-means, it is by no means clear whether our solutions reach the global minimum of the error function. Reaching the global minimum of clustering error is guaranteed only by making multiple runs of the algorithm, randomized for the number and initial values of cluster means, as well as the order of iteration of the data points; the solution corresponding to the minimum error value which also has the highest frequency of convergence may then be selected. In contrast to the random assignment of initial cluster means reported in (Jog et al., 2002), we used to select initial values by looking at

the data set, which may have compensated somewhat for lack of comprehensive testing for the minimization of global error.

Furthermore, the cluster solutions are probably distorted to some extent by the inclusion of outliers in clustering. Although we overestimate the initial number of clusters in order to trap outliers in separate clusters, it would make more sense to allow users to exclude egregious outliers from the clustering process and consider them for reinclusion in the cluster solutions later on the basis of their squared Mahalanobis distance from cluster means, waveform testing, and their effect on the cluster interspike interval histogram.

### *3.5.3.2 Alternative clustering algorithms*

For the K-means algorithm to work well, judicious but essentially ad-hoc choices must be made for the clustering parameter, the number of clusters, and the distribution of points within clusters. Bayesian classification methods, on the other hand, find the most probable form and number of classes in the data, and quantify the certainty with which each spike is assigned to a given class (Lewicki, 1994). However, a form for the cluster distribution must be chosen, and may be chosen to be anisotropic Gaussian. It might be better, however, to seek an automatic clustering algorithm which makes no assumptions about cluster distributions. Both (Fee et al., 1996a) and (Takahashi et al., 2003) employ hierarchical clustering methods in which the dataset is partitioned by some means into an overly large number of clusters, which are then reaggregated into a final set of clusters according to some criteria. (Fee et al., 1996a) reaggregate pairs of clusters based upon whether their cross-cluster interspike interval histogram shows a degradation in refractory period, and upon a “connection strength” between pairs of clusters which is related to the number of points along the boundary between the clusters. (Takahashi et al., 2003) decompose the initial clusters using independent component analysis to isolate somatic action potentials, and reaggregate pairs of clusters based upon the similarity of their ICBVs. (Independent component analysis is applicable because each cluster in the overclustered data set is likely to contain signals from fewer than four sources, the number of detectors in a tetrode.) Ultimately, the choice between Bayesian and hierarchical clustering methods depends upon whether for a given type of dataset it seems better to make an assumption about the cluster distribution or the appropriate clustering parameter. In particular, the phasically firing projection neurons of the striatum may produce markedly non-Gaussian clusters which would be more accurately separated using hierarchical methods.

### *3.5.3.3 Overlapping spikes and tetrode drift*

Our clustering method does not address overlapping spikes. Template matching might eliminate some data points composed of overlapping spikes, and overlapping spikes which are outliers may be manually eliminated in the clustering process, but it would be better to identify and decompose overlapping spikes so that they may be included in the clustering analysis and resulting spike trains. (Fee et al., 1996b) estimated the mutual entropy (information) between an observed waveform and the mean of its cluster as a function of the number of contiguous samples acquired per spike capture, and found that the mutual entropy is increased by only one bit between 14 and 32 samples, suggesting that spike captures could be reduced from ~1.3 ms to ~0.6 ms without much loss of spike discriminability. The shortened capture time would reduce the probability of components of more than one spike occurring within each spike capture. Alternatively, (Takahashi et al., 2003) decompose and classify overlapping spikes as part of the

clustering method described in the last section. The initial hierarchical clustering analysis is carried out only for the part of the dataset which may be fit by Gaussians centered around obvious cluster means; after it is completed, the outliers are segmented into a large number of clusters, decomposed via ICA into four components, and reaggregated based upon the similarity of their ICBVs. Some of the resulting clusters represent single action potential waveforms; those waveforms are subtracted from the spike captures of the remaining outlier clusters, and the decomposition and reaggregation are repeated on those remaining data until no more action potentials may be extracted. Finally, the clusters resulting from the outlier data are aggregated with the clusters resulting from the initial analysis according to the similarity of their ICBVs. In order to use Takahashi's method, no overlapping spikes can be eliminated from the dataset by template matching in the initial stage of analysis. Perhaps any point which best matches an MSN or TAN template should be retained for clustering, and non-MSN clusters should be eliminated afterward on the basis of their average waveforms and firing patterns.

We try to minimize tetrode drift by adjusting the tetrode level by small amounts and allowing time for the resulting position to stabilize before acquiring data. Of course, drift effects having to do with respiration are not compensated for by this method, and may affect the distributions of data points within clusters.

#### ***3.5.4 Isolation of unit firing across multiple days***

When tetrodes are left in the same place over several days, it is desirable to identify which clusters are attributable to the same source across days. Informally, clusters which are probably from the same source have remained fairly stable over as much as a week. (Schmitzer-Torbert and Redish, 2004) quantitatively identify clusters from the same source by computing the correlation (e.g., Pearson's correlation coefficient) of their mean vectors (in our case, the mean vector consists of the power measures on all four channels) and setting a criterion value. If a source drifts further (or closer) to the tetrode along its original direction from the tetrode, the correlation of its cluster to those of previous days will remain high; however, if it drifts in other directions, the ratios of power measures on the four channels will change, and resulting clusters will not be highly correlated with clusters from previous days.

### **3.6 Summary**

The general advantage enjoyed by tetrodes over single extracellular electrodes, that of superior separation of a larger number of sources near the electrode, makes a tetrode preparation uniquely suited for investigations of striatum. While there is as yet no conclusively apt description of striatal or, indeed, basal ganglia function, there is a great deal known about the anatomical organization of the striatum. Bridging of the gap between behavioral and anatomical results seems therefore to be the most viable approach to finding any commonality in seemingly disparate functionalities of the striatum (and basal ganglia). In this context, tetrodes make it possible for investigators to relate the activities of a group of neurons within a minimum 100-micron diameter sphere (Harris et al., 2000) to structural elements of up to roughly half a millimeter in diameter, and to the behavior of awake, unrestrained rodents. The modifications which have already been made to the original tetrode preparation in rodents (Gray et al., 1995) (strengthened tetrodes and reusable tetrode drives, in-vivo verification of tetrode locations and post-hoc reconstruction of source locations, and a modified cluster separation method) along with some further refinements (particularly the identification of clusters from the same source



across several days, and the adoption of a clustering technique which deals directly with overlapping spikes) should increase its effectiveness in the investigation of basal ganglia function.

## 4 Relating striatal learning to anatomy: a proposal

### 4.1 Background

In recent years, the focus in discussions of basal ganglia function has shifted from their presumed modulation of motor control parameters to their involvement in procedural or “habit” learning. Since habits may be motor or non-motor, it is tempting to hope that the common transformation performed on all input by the basal ganglia may be characterizable by this high-level description (Graybiel, 1998). The dorsal striatum (caudate nucleus and putamen) is implicated in human procedural learning by deficiencies in patients with Huntington’s and Parkinson’s diseases relative to healthy people. Tasks used to probe procedural learning in humans include acquisition of probabilistic relations between cues and outcomes, and learning sequences “hidden” in presentations of visual stimuli to which motor responses are required (Knowlton et al., 1994; Laforce and Doyon, 2001). In the weather prediction game of (Knowlton et al., 1994), patients are impaired in learning to predict sunny versus rainy weather given combinations of four geometric cues which are probabilistically related to each outcome. On the other hand, temporal lobe amnesic patients perform normally on this task, confirming the intuition that it does not depend on declarative learning and memory processes. In neuroimaging studies with normals, similar procedural learning tasks reveal activation in the caudate nucleus in correlation with acquisition, which activation furthermore does not occur when the subjects are explicitly informed of the underlying rule beforehand (Doyon et al., 1996; Jueptner et al., 1997; Rauch et al., 1997; Jueptner and Weiller, 1998).

In rodent and primate studies, procedural learning is commonly translated into learning of stimulus-response associations, which follows an analogously slow timecourse and may be characterized as formation of “habitual” responses to stimuli. In primate studies, sequence learning tasks requiring saccade or arm/hand/finger responses to successively presented stimuli are often used, but differ from human sequence learning tasks; the sequences are overtly presented, and learning of the sequence is specifically interpreted as learning a chain of stimulus-response associations. Results of such studies can be related to reports of motor sequence learning related activity in primate presupplementary and supplementary motor cortical areas, which are output areas of the proposed “motor” cortico-basal ganglia circuit (Tanji et al., 1996). Projection neurons in the caudate nucleus of primates have been demonstrated to fire in association with one or multiple phases in sequences of eye and eye-hand movements. Moreover, the sequence-related firing is sequence-specific (Kermadi and Joseph, 1995; Kimura et al., 1996; Miyachi et al., 2002). In rodents, the only well-defined association between sequences and the striatum has been made for *instinctive* four-phase grooming sequences; neurons in a well-defined area of dorsolateral striatum respond to one or two phases of the chain, but not to similar movements in non-chain grooming sequences, indicating sequence specificity. Furthermore, it is indicated that the striatal grooming area is not necessary for initiation of this “syntactic” grooming or for basic grooming movements, but for correct implementation of the

four-phase sequence. Finally, firing specifically associated to phases of the grooming sequence has been found in SNr (Berridge, 1989; Cromwell and Berridge, 1996; Aldridge and Berridge, 1998; Meyer-Luehmann et al., 2002). These findings strongly suggest further directions for investigation of neuronal activity associated with learned sequences in basal ganglia.

Most rodent studies of stimulus-response learning have focused on lesioning putatively involved brain areas and looking for deficits in acquisition of single stimulus-response associations. Double dissociation studies have differentiated dorsal striatal versus hippocampal involvement in pairs of tasks which differ only in the learning and memory mechanism required for acquisition: working memory/visuospatial associations (dorsal hippocampus) versus stimulus-response learning (dorsal striatum). The win-stay task, in which rats must visit four cued maze arms twice within a session, utilizes the same 8-arm radial maze as the hippocampal-dependent win-shift task, in which all of the maze arms must be visited only once (Packard et al., 1989). Similarly, a water maze task in which the location of a submerged platform is cued by a ball with a visual pattern regardless of its location is dissociable from a hippocampal-dependent version in which the location of the submerged platform remains constant regardless of the visual pattern on the cue ball (Packard and McGaugh, 1992). The nature of learned responses – whether rats learn to go “to” a cued place or to take a specific action – is further clarified by studies which dissociate goal places from response actions. For example, (Packard and McGaugh, 1996) trained rats to enter the “south” arm of a plus-maze and make a left turn into the “west” arm for reinforcement. In probe trials on day eight and sixteen of training, rats were put in the north arm to see whether they had learned to go into the west arm, or to make a left turn. Control rats went to the west arm on day eight, indicating learning of goal place, and made a left turn on day sixteen, indicating a shift to learning of a response. On the other hand, rats receiving lidocaine injections in the dorsolateral caudate or dorsal hippocampus just before probe trials showed blockade of the expression of response learning and place learning, respectively.

One criticism of the above rodent studies is that their tasks are not easily comparable with human procedural learning tasks. (Christie and Dalrymple-Alford, 2004) have defined a sequence-learning task analogous to the serial reaction time task in humans, in which rats with lesions of dorsal caudate nucleus are impaired in learning a sequence of more than four cued nose-pokes. The task uses nose-poke holes at four locations, allowing use of varying sequence lengths. Moreover, blocks of several trials may be run per training session, allowing within-session switching from learned to random sequences in order to verify sequence specificity of learning by observing increased reaction times and errors as in the human version of the task.

Recent work has begun to differentiate functions of rodent dorsolateral versus dorsomedial striatum. For example, dorsomedial striatum is thought to be involved in behavioral flexibility, that is, the inhibition of former response strategies and the facilitation of learning of new responses to match a shift in conditions (Sakamoto and Okaichi, 2001; Ragozzino et al., 2002; Ragozzino, 2003). Moreover, rats with dorsolateral but not dorsomedial striatal lesions which are trained to press a lever on an interval reinforcement schedule refrain from lever pressing after the reinforcer is devalued by pairing with nauseating lithium chloride injections, indicating involvement in (motor) habit formation of dorsolateral but not dorsomedial striatum (Yin et al., 2004). These functional differences reflect the pattern of projections from cortical areas to striatum; somatosensory and motor cortices project to dorsolateral striatum, while sensory cortices and frontal and cingulate areas project to the dorsomedial sector (McGeorge and Faull, 1989). Therefore, lesion studies of dorsal striatal association with aspects of behavior need to

target specific sub-areas of dorsal striatum, which may be part of different cortico-basal ganglia loops.

In rodents, then, the dorsolateral striatum, which forms at least part of the striatal substrate for stimulus-response learning, is also the area of striatum for which the organization of cortical inputs to medium spiny projection neurons is most clearly understood (see section 2). It is often assumed that the somatotopy of dorsolateral striatum, inherited (albeit with transformation and recombination) from the somatotopy of somatosensory and motor cortical areas, forms a substrate for elemental building blocks of learned (single and sequences of) motor responses. Yet no studies have correlated S-R learning-associated dorsolateral striatal neural activity with specific activation of representations of body parts involved in the learned responses. Nor has such neuronal activity been registered with striosomal and matrix boundaries. Tetrodes, which record the activity of local groups of neurons at spatial scales comparable to striosomes and body part representations, provide a viable method for not only observing the responses of large numbers of neurons over S-R learning, but also for investigating whether and how neuronal activity changes in striatum which are correlated with S-R learning occur in relation to these anatomical features.

(Jog et al., 1999) indeed used tetrodes to observe S-R learning-correlated neuronal activity changes in medium spiny neurons of dorsolateral striatum. Three rats were trained to turn left or right on a T-maze given a 1-kHz or 8-kHz cue tone. On average, 30 units were recorded per day over 2-3 weeks from 3 rats. Over task acquisition, the percentage of recorded units which had task-related responses increased from 56% to a maximum of 92%. (Task-related responses were defined as significant increases in firing rate in close temporal correlation with some phase of the task relative to a within-neuron baseline firing rate.) Meanwhile, the percentage of neurons responsive to the left and right turns dropped from 65% to 13% by the end of training. Concurrently, the percentages of neurons active at the start and/or goals of the T-maze increased greatly; start-related units increased from 44% to 88%, and goal-related units increased from 29% to 67%. (Over training, the numbers of units responsive to multiple task events increased from 44% to 70%.) The percentage of cue tone-responsive neurons stayed very low, except in one of the rats in which the tetrodes had a more medial placement within striatum. The reported percentages were averaged across all rats, but reflect the trends within individual subjects. These results seem to suggest that as S-R learning progresses, neural activity related to the response being learned disappears, as neural activity related to aspects of the context in which the response is to be generated increases, in dorsolateral striatum of rodents. (Tetrode implantation site was AP = +0.5, ML = +3.7 mm relative to bregma.)

Since the publication of this experiment, (DeCoteau et al., 2000) have verified that acquisition of the cued T-maze task is impaired in subjects with ibotenic acid lesions of dorsolateral striatum. Intact rats were trained until the learning criterion was reached, and probe trials (using an entrance arm opposite to the usual entrance arm) demonstrated that the rats learned to make responses (left or right turns) rather than to go to particular maze ends. Rats were then lesioned and retrained for 10 days. Daily probe trials during retraining demonstrated that lesioned animals learned to go to goal places rather than to make responses, and that their performance never reached the level of that of rats with sham lesions. This study not only confirms the necessity of an intact striatum to perform the task, but also confirms that what is learned are turn responses, i.e., that it is indeed an S-R learning task.

There remains much to understand about the results of (Jog et al., 1999). For example, the researchers did not control for non-learning-specific changes in neuronal recruitment. This could have been done by defining a control task with similar sensory, motor, and motivational parameters which does not require S-R learning, such as a delayed alternation task. Additionally, the nature of the “start” and “goal”-responsive neuronal activity is ambiguous; “start” activity was defined as related to “start-gate opening or initiation of locomotion” (Jog et al., 1999), and “goal” events were defined at spatial and temporal locations just adjacent to the locations of visible (chocolate) reinforcement, so that it is unclear to what extent “goal”-responsive neuronal activity is related to perception or consumption of reinforcement. Similarly, “start” activity could perhaps be related to memory of recent reception of reinforcement, or to formation of reference memory of reinforcement presence at the end of the maze path (which would seem to involve a type of place coding). The researchers did look for formation of stereotypic motor responses at maze ends, and correlations of firing rates at maze ends with acceleration and deceleration at start and goals, and found no relationship between these factors and the changes of “start” and “goal” activity over the training period. It is interesting that (Hu et al., 2001) observed that when rats are overtrained by an additional 10 sessions, “start” and “goal”-related neuronal activity decreases.

As turn responses involve the whole body, it was not possible to observe whether S-R learning-related activity appeared only in representations of body parts involved in the response. Nor were the positions of tetrodes compared to striosomal boundaries. Indeed, the activity occurring at the ends of the maze, and perhaps the cue tone-related activity, might have been specific to striosomal neurons. (Schmitzer-Torbert and Redish, 2004), in recording activity with tetrodes from dorsolateral striatum of rats as they learned to run a multiple T-maze which formed a four-turn sequence, found that neurons which responded as the rats ran on the maze and neurons which were correlated with receipt of reinforcement were two separate populations. This result aligns well with anatomical and functional distinctions of striosomes and matrix; however, the researchers did not attempt to localize tetrodes with respect to striosomal boundaries.

(Jog et al., 1999) were not able to determine to what extent clusters recorded in different daily sessions came from the same units. Moreover, although some tetrodes were not moved over the 2-3 week recording periods, others were moved by hundreds of microns. Thus it could be possible that the changes in neuronal recruitment observed over the training period were at least partly due to sampling of different neuronal populations (i.e. turn-related vs. start or goal-related). Also, it was not possible under these conditions to observe whether the shift from motor to non-motor related activity occurred within single units.

The only other study of dorsolateral striatal neuronal responses during S-R acquisition agrees with (Jog et al., 1999) in reporting a decrease of neuronal activity correlated with a cued lever-press over the course of task acquisition (Carelli et al., 1997). The lever press was performed with the right forelimb, from a consistent starting point and posture, in response to a 1-kHz auditory cue. The lever was calibrated to the amount of applied force, with water reinforcement delivered upon application of a given force so that “efficiency” of lever press (i.e., application of sufficient, but not excessive force) could be measured over the learning period. Lever-press “efficiency” did increase over learning; however, two-thirds of “lever-press-related” activity was in correlation with the initial reach toward the lever rather than the depression of the lever, which disqualifies increase in lever-press efficiency as the correlate of the decreased neuronal

activity. In addition to using a well-controlled movement of an isolated body part, the researchers recorded from neurons which responded to cutaneous stimulation and passive movement of only the right forelimb. This measure demonstrates S-R learning activity changes in neurons responsive to sensorimotor manipulation of the involved body part, but does not eliminate the possibility that S-R learning activity changes also occur in neurons which are responsive to sensorimotor manipulation of other body parts. (This group of researchers ascertained in earlier studies that unit activity found at single sites in the striatum is responsive to cutaneous stimulation and passive manipulation of one and only one body part – e.g., (Cho and West, 1997).) Furthermore, no study since (Liles and Updyke, 1985) has attempted to verify that body-part manipulation responsive neurons register with anatomically-defined body part areas.

If functionally-defined body part areas may be identified with anatomically-defined body part areas, it may explain why (Carelli et al., 1997) do not report activity at task events analogous to the “start” and “goal” events of (Jog et al., 1999). Body part areas as defined by anterograde anatomical tracers from cortex are input matrixomes. If “start” and “goal”-related activity occurs only in striosomal populations, it would not be observed in this study.

(Carelli et al., 1997) recorded from 53 dorsolateral striatal neurons (AP = +0.80, ML = +3.6 or +4.0 mm relative to bregma) related to forelimb manipulation and aspects of the lever press task, across three rats, and observed that the firing rate in 21 of these neurons was significantly increased in close temporal correlation to the initial reach toward the lever and/or lever depression, relative to a baseline firing rate defined within the same neurons while the rat was in a standardized stationary position prior to lever-press initiation. 20 of these neurons were recorded during the first 9 days of training, while only one was recorded during the second 9 days of training (with a total of 18 training days). No cue tone-related activity was observed in later sessions. As the researchers introduced and retracted their electrode each day, it was not possible to track activities of the same neurons over the training period; therefore the observed differential of activity related to lever press might be partly due to a sampling effect. Moreover, within-neuron activity changes over learning could not be observed. Given the definition of firing-rate changes as significant relative to pre-movement baseline activity, it is possible that an increase in baseline firing rates over learning (something like “start”-related activity) could account for failure to see significant firing rate increases time-locked to lever press in later training sessions. However, the paper presents peri-event histograms centered around lever press events for neurons recorded on early and late training days which show lack of time-locked firing of the late-day neurons to lever press.

Finally, although the cued lever-press task seems to be designed to involve stimulus-response learning, this assumption has not been verified. In addition, neuronal activity changes occurring with learning of the cued lever-press task should be compared with neuronal activity changes occurring with learning of a control task which has similar sensory, motor, and motivational parameters but does not require S-R learning.

It is interesting to compare the studies of (Jog et al., 1999) and (Carelli et al., 1997) with that of (Gardiner and Kitai, 1992). They put single electrodes into dorsolateral striatum (AP = -0.7, ML = +3.5 mm relative to bregma) *after* rats were trained to turn their heads left or right in response to a tone (800 Hz, 25 ms) from the desired direction. The head turn, like the lever press of (Carelli et al., 1997), was well-controlled; rats had to insert their heads through a 35-mm hole and hold still with head straight ahead in order for a cue tone to be initiated. Either IR detectors in the floor, or EMG onset time of sternomastoid or cleomastoid muscle activity

defined the beginning of head turn, while end of the head turn was defined by breakage of IR detectors located just in front of reinforcement spouts (glucose-saccharine solution), located 25 mm from midline. Rather than observing a relative lack of movement related to head turning, the researchers found single units with firing rates that significantly increased in close temporal correlation with head turns relative to a within-neuron baseline which was the average of firing activity during a 500 ms period in which the animal was still before tone cue presentation. Some units were responsive to the tone cue and/or head turning. All tone cue responses disappeared or decreased if access to the head hole was blocked, indicating context-dependence of tone cue-related activity on the relation of cue to an upcoming response to be made. Not only were recordings not specifically taken from neurons responsive to cutaneous stimulation or passive movements of neck, the researchers describe a unit which fired in association with task related movements to the right, but was not responsive to tactile stimulation or passive movements of neck (or head, orofacial areas, or limbs). Nor did this neuron fire in relation to spontaneous head movements to the right, thus demonstrating context-specificity of firing to cued responses. 54 task-related units were recorded across 12 rats. Task-related neurons were not localized relative to striosomal boundaries. As with the two preceding studies, it has not been verified whether the task is dependent on stimulus-response learning; nor are observed neuronal activity changes compared to activity correlated with learning of a control task with similar sensory, motor, and motivational elements to control for activity unrelated to S-R learning.

Neuronal activity was also observed in many neurons during the period of reinforcement consumption in 20 units; for 11 of them, the responses only occurred at the left or right reinforcement spouts. Moreover, most of the activity lasted for less than 500 ms, in contrast to the roughly 2-5 s duration of spout licking activity. The researchers present raster plots of activity of one unit in which a single spike occurs after reinforcement delivery on each trial, at what looks like a very consistent interval after head movement onset. This single spike looks like an explicit signal of “response end,” and indeed, with the introduction of a delay between the end of head turn and the delivery of reinforcement, it may be possible to characterize neuronal activity signaling the end of a learned response, in the way that (Fujii and Graybiel, 2003) have described activity in macaque prefrontal cortical neurons which seems to signal the beginning and end states of learned sequences of saccades to cued targets (including sequences of length 1).

A notable difference between the protocol of this study and the preceding two studies is in the stereotaxic coordinates of electrode entry. While (Jog et al., 1999) and (Carelli et al., 1997) have implantation sites at AP = +0.5 and +0.80 mm relative to bregma, (Gardiner and Kitai, 1992) make their opening at AP = -0.7 mm relative to bregma, and record neurons from sites ranging from AP = 0 to -1.5 mm relative to bregma. Interestingly, the disappearance in the former two studies and the retention in the latter study after acquisition of learned motor response-related neuronal activity seems to parallel results in primates (Miyachi et al., 1997; Miyachi et al., 2002) and humans (Jueptner and Weiller, 1998) which indicate an anterior/posterior double dissociation of activation in striatum related to learning of new motor responses (sequences) and performance of learned responses. But in humans and primates, “anterior striatum” refers to the caudate nucleus and anterior putamen rostral to the anterior commissure, and is known as the “association striatum” because it receives inputs from frontal association areas (Miyachi et al., 2002). “Posterior striatum” refers to the caudal putamen, which receives projections from sensorimotor cortices, and thus corresponds to dorsolateral striatum in rodents. In contrast, the “anterior” and “posterior” sites in the three rodent studies are both located within the

rostrocaudal extent of the dorsolateral “sensorimotor” striatum (McGeorge and Faull, 1989; Cho and West, 1997), and are separated in relation to bregma, which is roughly 2.5 mm rostral to the anterior commissure (Thompson, 1978). “Association” striatum is medial to sensorimotor striatum in rodents (McGeorge and Faull, 1989). Although the tetrode implantation site of (Gardiner and Kitai, 1992) is a few hundred microns medial to those of the two S-R acquisition studies, the lateral extent of the recording sites might have been greater in this study. Alternatively, there may be a greater presence of striosomes or TAN’s in anterior versus posterior dorsolateral striatum, although there seem to be no reports of such differentiations.

In addition to recording from striatal neurons, (Gardiner and Kitai, 1992) also recorded task-related unit activity in the globus pallidus (corresponding to primate GPi) and found activity changes in correlation with both head movements in specific directions and tone cues, with cue responses mostly specific to subsequent head turns as for dorsolateral striatal units. Some units also had activity which occurred during the consumption of reinforcement, with response characteristics similar to striatal units. A few units were observed to respond exclusively to cued or spontaneous head turns. No topographic organization was observed. Interestingly, bursting and pauses were observed during the rats’ exploratory behavior and grooming, which might be activity related to onset of phases of the stereotypic four-phase grooming sequence similar to that observed in SNr by (Meyer-Luehmann et al., 2002). Activity related to movement preparation and phases of a learned elbow flexion sequence, consisting of both increased and suppressed firing, has also been observed in GPi of macaque monkeys by (Kimura et al., 1996). Activity in GPi during acquisition of a single motor response or sequence of responses has not been studied.

In light of the similarities and differences in the results from (Jog et al., 1999), (Carelli et al., 1997), and (Gardiner and Kitai, 1992), which employ very analogous tasks, it would be interesting to register the three tasks with a common structure of task events, verify their dependence upon an intact dorsolateral striatum and establish non S-R control tasks with similar sensory, motor, and motivational elements, and record with tetrodes from dorsolateral striatal neurons at the same sites anterior and posterior to bregma within subjects as they learn one of the tasks or control tasks. Use of tetrodes is expected to increase the overall yield of recorded units and thereby the yield of task-responsive units; compare the sample size reported by (Jog et al., 1999) to those reported by (Carelli et al., 1997) and (Gardiner and Kitai, 1992). Moreover, the recorded units are in local groups on the spatial scale of striosomes or body part areas in matrix. Recording from both anterior and posterior sites within subjects over task acquisition would allow the observation and comparison of the time courses of neuronal activity changes in these areas over the course of S-R learning. Furthermore, locations of tetrodes recording neurons responsive to the S-R tasks could be localized relative to striosomal borders by histological methods. Units with reinforcement-related activity (if found) might be located in striosomes. In the forelimb and neck-specific S-R tasks, task responsiveness of involved and non-involved body part-responsive neurons identified by cutaneous stimulation and passive manipulation could be compared; these recording sites could then be localized relative to body part areas identified by anterograde tracers injected into motor cortex. Finally, neuronal activity could be recorded from GPi and SNr over acquisition of S-R and control tasks, to look for S-R learning-specific activity changes in basal ganglia output areas. This set of experiments would begin the attempt to make an explicit mapping between S-R learning-related neuronal activity and the sensorimotor somatotopy and compartmental organization of the dorsolateral striatum. Additionally, the important question of whether or not neuronal activity correlates to S-R learning occur in basal ganglia output areas would be addressed.

## 4.2 Specific Aims

1. Verify dorsolateral striatal dependence of one T-maze task and two body part specific tasks which are thought to require stimulus-response learning and establish control tasks which have similar sensory, motor, and motivational but not learning requirements.
2. Arrive at a consistent description of how dorsolateral striatal neuronal activity at levels anterior to bregma changes in correlation with stimulus-response learning occurring in one T-maze task and two body part specific tasks, relative to control tasks which have similar sensory, motor, and motivational but different learning requirements.
3. Arrive at a consistent description of how dorsolateral striatal neuronal activity at levels posterior to bregma changes in correlation with stimulus-response learning occurring in one T-maze task and two body part specific tasks, relative to control tasks which have similar sensory, motor, and motivational but different learning requirements. Compare the time course of changes in anterior and posterior striatal activity with learning within subjects.
4. Investigate whether stimulus-response learning-related neuronal activity changes occurring in two body part specific tasks appear only in striatal neurons responsive to cutaneous stimulation and/or passive manipulation of the involved body part.
5. Localize neurons responsive to sensorimotor and other parameters in stimulus-response learning relative to striosomes and matrix.
6. Verify registration of striatal neurons responsive to specific body part stimulation with body part representations identified by anatomical tracers.
7. Demonstrate presence or absence of activity changes in basal ganglia output areas (GPi and SNr) in correlation with stimulus-response learning occurring in one T-maze task and two body part specific tasks, relative to control tasks which have similar sensory, motor, and motivational but not learning requirements.

## 4.3 Experimental design and methods

### 4.3.1 Task designs

The cued-arm T-maze task of (Jog et al., 1999) allowed the observation of an increase in neuronal recruitment in levels of striatum anterior to bregma at the beginning and end points of the learned T-maze responses over the course of acquisition, in addition to the disappearance of sensorimotor-related firing which was first demonstrated by (Carelli et al., 1997) for a cued lever-press task. On the other hand, (Gardiner and Kitai, 1992) demonstrated the retention of sensorimotor-related firing in levels of striatum posterior to bregma after acquisition of a cued head movement task. Standardizing the structure of the three tasks and analysis of resulting neuronal and behavioral data will hopefully yield a consistent picture of how neuronal activity patterns in the striatum at anterior and posterior levels and in basal ganglia output areas change over the course of acquisition of three stimulus-response habits which employ different body parts.

The task and analysis structures are based upon those used in (Jog et al., 1999) for the cued T-maze task, designed to examine changes in the percentages of recorded neurons responsive to



various significant task phases as the task is learned. In the original experiment, “Start,” or the initiation of movement, is defined by the breaking of a photobeam pair placed just after the starting gate; “Tone Onset” of a 1-kHz or 8-kHz tone signaling left or right turn occurs when a second photobeam pair is broken midway down the maze arm; “Action Onset,” or the beginning of a right or left turn, is estimated by the breaking of a third photobeam pair; “Action Offset” by a fourth pair; and “Goal” is defined by the breaking of a photobeam pair at the end of the maze, placed just before a food reinforcement. To better examine the “Start” and “Goal” related neuronal activity which emerges as the T-maze task is learned, two other events are defined: “Begin Trial,” synchronous with release of the starting gate, and “Reinforcement,” synchronous with delivery of reinforcement, which will be delivered at some delay after “Goal” is reached. The lever press and head movement tasks of (Carelli et al., 1997) and (Gardiner and Kitai, 1992) are modified to register with this structure (Table 1). For all three tasks, reinforcement is juice delivered from spouts, which allows control over the time of reinforcement delivery and regularizes visual and olfactory cues in correct and incorrect goal choices.

The original cued-lever press task of (Carelli et al., 1997) involved learning to press one lever in response to a cue tone. Here there are two tones and two levers, in analogy with the T-maze and head movement tasks, allowing the definition of delayed alternation versions of all three tasks, whose appropriateness as control tasks will be tested (see section 4.3.3). The rat learns to stand still with left forepaw flat on a piece of tape placed in front of two calibrated force levers, and press the appropriate lever given a 1-kHz or 8-kHz tone (Figure 8). “Begin Trial” is synchronous with the release of an opaque wall blocking vision of and access to the levers; “Start” is defined as the time at which the rat places its left forepaw flat on the designated spot and holds still for 1 second; “Tone Onset” occurs at the end of that second; “Action Onset” is defined as the initiation of lifting the paw from the starting posture, determined by the time of biceps or deltoid EMG onset; “Action Offset” is not distinct in this task from “Goal,” which is defined as the time at which the lever press reaches sufficient force to initiate reinforcement; and “Reinforcement” occurs at some delay after “Goal” is reached.

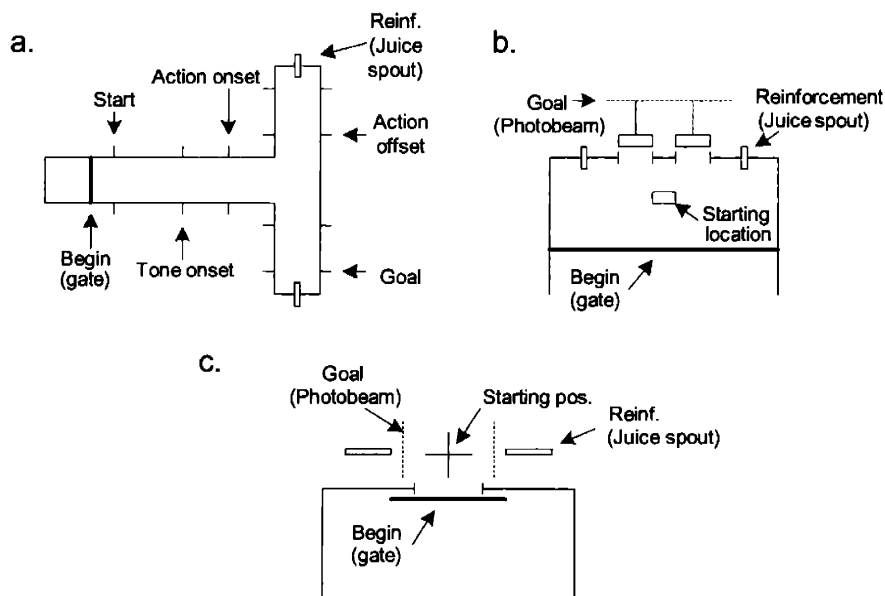


**Figure 8: Task apparatus. (a) T-maze. (b) Lever-press chamber. (c) Head-movement chamber.**

The head movement task of (Gardiner and Kitai, 1992) involves putting the head through a narrow window and holding still for 1 second, causing initiation of a tone from the left or the right which indicates the direction of head turn to obtain reinforcement (Figure 8). Here, two tones are used, and initiated from the same direction (straight ahead), in analogy with the T-maze and lever-press tasks. “Begin Trial” is synchronous with the release of a gate which reveals the opening in the wall; “Start” is defined as the time at which the rat places its head through the opening in the wall and holds still for 1 second; “Action Onset” is defined by the breakage of photobeam or IR detectors, or by the time of sternomastoid or cleomastoid onset; “Action Offset” is not distinct in this task from “Goal,” which is defined as the time of breakage of photobeam or IR detectors placed just in front of the location of reinforcement delivery; and “Reinforcement” occurs at some delay after “Goal” is reached.

The design of the three tasks easily allows definition of delayed alternation tasks with similar sensory, motor, and motivational but different learning requirements as putative control tasks. For the T-maze task, there is no “Tone Onset”; for the other two tasks, which require holding a consistent starting posture before the action, a tone must be used to signal the end of the required “still” period. A brief, low-volume 1 kHz tone is therefore used for all trials in the delayed alternation lever-press and head movement tasks. If it is possible to train the rats to hold still for the required period before taking action in the delayed alternation tasks, the cue may be eliminated.

In order to further investigate the increase of neuronal recruitment in anterior striatum at the beginning and end points of the T-maze actions over learning which was observed by (Jog et al., 1999), the delay between “Goal” and “Reinforcement,” the amount of reinforcement, and the intertrial interval will be varied in rats which have acquired that task. If beginning and end point activity is observed in rats over learning of the other two tasks, these parameters will be varied for those subjects as well.

| <b>Event</b>         | <b>T-Maze</b> | <b>Lever-Press</b>          | <b>Head movement</b>                   |
|----------------------|---------------|-----------------------------|--|
| <b>Begin Trial</b>   | Open gate     | Open gate                   | Open gate                              |
| <b>Start</b>         | Photobeam 1   | Paw on tape                 | Head through window                    |
| <b>Tone Onset</b>    | Photobeam 2   | Start posn. for 1.0 s       | Start posn. for 1.0 s                  |
| <b>Action Onset</b>  | Photobeam 3   | Biceps/deltoid<br>EMG onset | Sternomastoid/cleomastoid<br>EMG onset |
| <b>Action Offset</b> | Photobeam 4   | Same as goal                | Same as goal                           |
| <b>Goal</b>          | Photobeam 5   | Force-bin 3 entry           | Detectors                              |
| <b>Reinforcement</b> | After delay   | After delay                 | After delay                            |

**Table 1: Task structures.**

### 4.3.2 Task-specific methods

#### 4.3.2.1 Cued and delayed alternation T-maze tasks

*Task apparatus and procedures:* Both tasks employ a T-maze like that of (Jog et al., 1999), with photobeam pairs placed at spatial intervals to mark the initiation of locomotion after release of the starting gate (“Start”), initiation of cue tones for the cued-arm task (“Tone Onset”), initiation and completion of left and right turns (“Action Onset” and “Action Offset”), and the ends of the maze (“Goal”). Additionally, the times of starting gate release (“Begin Trial”) and reinforcement delivery (“Reinforcement”) are noted. Gate opening, reinforcement delivery, and recording of the seven task event times are computer-controlled. The juice spouts located at maze goals may be set to deliver juice at a variety of intervals after breakage of the “Goal” photobeam pair using a time delay relay (e.g., Davis-Inotek, TR series). Each trial of either task is initiated by the release of a starting gate and terminated by breakage of a “Goal” photobeam pair. In the cued task, a 1-kHz or 8-kHz tone (75 dB) is issued upon breakage of the “Tone Onset” photobeam pair, instructing the rat to turn left or right, respectively, and terminating upon breakage of a “Goal” photobeam pair. In the delayed alternation task, no tone cue is used. Before a training session is initiated, juice is run through the spouts to equalize any olfactory cues at the maze endpoints. Trials are run in everyday light, with the maze surrounded by a Faraday cage lined with black paper. A videocamera is mounted overhead to monitor and acquire a visual record of subjects’ behavior.

In neuronal recording experiments, the computer which controls gate opening, tone initiation and reinforcement delivery and detects photobeam breakages sends messages to the acquisition computers when these events occur, triggering annotation of the neuronal data stream. The behavioral video acquired by a ceiling-mounted camera is juxtaposed with the timestamps of the acquisition software by means of a video mixer.

*Pretraining for both tasks:* As per (Jog et al., 1999), three to five preliminary sessions will be given to acclimate subjects to the maze, until the rat leaves the start area within 10 seconds after start gate opening and walks down the track in 5 consecutive trials. For each subject, one session is given per day, consisting of 40 trials. In this phase, no tones are used, and subjects may obtain reinforcement at both goals.

*Training for the cued-arm task:* Each subject is given one training session per day, consisting of 40 trials, 20 for each tone presented pseudorandomly. Training continues for 7-10 days of overtraining after rats first reach the 72.5% correct criterion for acquisition, for a total training time of 14-21 days (Jog et al., 1999). Lesioned rats are trained for a comparable length of time. Trials in which the rat does not enter one of the endpoints within 2 minutes of start gate opening are scored as errors.

*Training for the delayed alternation task:* Each subject is given one training session per day consisting of 40 trials. As with the cued-arm task, training continues for 7-10 days after first rats reach the 72.5% correct criterion for acquisition. Lesioned rats are trained for a comparable length of time. Trials in which the rat does not enter one of the endpoints within 2 minutes of start gate opening are scored as errors.

#### 4.3.2.2 Cued and delayed alternation lever-press tasks

*Task apparatus and procedures:* The lever-press tasks are structured to register with the T-maze tasks described above, with analyses of neuronal activity responsive to blocking wall removal ("Begin"), initiation of the starting posture ("Start"), initiation of cue tones ("Tone Onset"), lifting of the paw to lever press ("Action Onset"), end of lever press ("Goal"), and delivery of reinforcement ("Reinforcement"). Both tasks employ an experimental chamber based upon that described in (Carelli et al., 1997), made of clear Plexiglas with flooring of the same material as the T-maze. Dimensions of the chamber are 32 cm L x 17 cm W x 40 cm H. One wall of the chamber is movable, with two rectangular openings approximately 2 x 2 cm each, separated by a narrow Plexiglas divider. The wall may be moved to expose or retract two levers mounted 4 cm from the floor. The rectangular openings must be spaced so that the rat does not turn in addition to extending the paw in order to press the levers. A juice spout is mounted 6 cm to the side of each lever for delivery of reinforcement. An opaque black Plexiglas wall is removed at the beginning of each trial to allow access to the levers and juice spouts. Each lever is calibrated to the amount of force applied by the rat as in (Carelli et al., 1997), by conversion via a transistor circuit of the extent to which the lever interrupts a photobeam positioned behind it into five increments in force applied to the lever. Those increments are defined as follows: bin 1 (1-5 gm), bin 2 (6-10 gm), bin 3 (11-15 gm), bin 4 (16-20 gm) and bin 5 (21-25 gm). The time of bin 1 entrance is taken as the initiation of lever press. Entry into bin 3 defines the end of lever press ("Goal"). Removal of the wall, reinforcement delivery, and recording of bin entrance times are computer-controlled. The juice spouts may be set to deliver juice at a variety of intervals after breakage of the "Goal" detector using a time delay relay (e.g., Davis-Inotek, TR series). Once a trial is initiated by removal of the black blocking wall, the animal is required to stand facing the levers with the left forepaw placed flat on a piece of tape located 1.5 cm from the central divider. In the cued lever-press condition, if the animal maintains this position for 1 second without moving (as determined by the experimenter or motion detectors), a 1 or 8 kHz tone (75 dB) is issued which instructs the rat to press the left or right lever. In the delayed alternation condition, a brief, low-volume 1 kHz tone is used in order to instruct the rat to initiate movement toward lever press. As in (Carelli et al., 1997), reinforcement delivery is contingent upon initiating lever press within 7 seconds of tone onset. Tone offset in the cued condition is synchronous with entry into bin 3 ("Goal"). Before a training session is initiated, juice is run through the spouts to equalize any olfactory cues. Trials are run in everyday light, with the experimental chamber surrounded by a Faraday cage lined with black paper. A videocamera is mounted to monitor and acquire a visual record of subjects' behavior.

In neuronal recording experiments, the computer which controls removal of the blocking wall, tone initiation and reinforcement delivery and detects entry into bin 3 ("Goal") sends messages to the acquisition computers when these events occur, triggering annotation of the neuronal data stream. The behavioral video is juxtaposed with the timestamps of the acquisition software by means of a video mixer. Initiation of the starting posture ("Start") must be determined by examination of timestamped behavioral video.

*Pretraining for both tasks:* Animals are initially trained to press either lever with the left forepaw to enter bin 3 and obtain reinforcement. The levers are gradually retracted to 5 mm behind the movable wall, requiring rats to reach through the holes in the wall with the left forepaw to lever press (Carelli et al., 1997). At this point the blocking wall is introduced, and

rats are trained to initiate lever press from the starting position with left forepaw on the tape. In this phase, no tones are used.

*Training for cued-lever press:* Each subject is given one training session per day, consisting of 70 trials, 35 for each tone presented pseudorandomly. (Carelli et al., 1997) report that 2 of their 3 rats reached 90% correct performance around day 6 or 7, and that each rat was trained for 18 days. The current task, which requires acquisition of two stimulus-response associations rather than one, may take longer to acquire. Rats will be trained for 7-10 days after first reaching the 72.5% correct criterion for acquisition (Jog et al., 1999). Lesioned rats will be trained for a comparable number of days. Trials in which the rat does not enter the starting position within 1 minute after the blocking wall is removed are scored as errors. Extra lever presses are scored as errors. Lever presses which are not initiated from the correct starting position and cued by the tones are scored as errors.

*Training for delayed alternation:* Each subject is given one training session per day consisting of 70 trials. As with the cued lever-press task, training will continue for 7-10 days after rats first reach the 72.5% correct criterion for acquisition. Lesioned rats are trained for a comparable number of days. Trials in which the rat does not enter the starting position within 1 minute after the blocking wall is removed are scored as errors.

#### 4.3.2.3 Cued and delayed alternation head movement tasks

*Task apparatus and procedures:* The head movement tasks are structured to register with the T-maze tasks, with analyses of neuronal activity responsive to starting gate release (“Begin”), initiation of the starting posture (“Start”), beginning of head turn (“Action Onset”), end of head turn (“Goal”), and delivery of reinforcement (“Reinforcement”). The rat is placed in a small transparent Plexiglas training chamber with flooring of the same material as in the T-maze and lever-press chamber and a 35 mm W x 1 cm H opening in one wall, after the method of (Gardiner and Kitai, 1992). Two juice spouts are placed 25 mm laterally to the right and left of the opening. Infrared detectors or photobeam pairs are used to monitor head position, so that placement on the midline (“Start”) and finish of head turns (“Goal”) are defined by occlusion of detectors. Trials are initiated by the release of a starting gate (“Begin”) to reveal the opening. Release of the starting gate, delivery of reinforcement, and recording of detector breakage times are computer-controlled. The juice spouts may be set to deliver juice at a variety of intervals after breakage of the “Goal” detector using a time delay relay (e.g., Davis-Inotek, TR series). Each trial of either task is initiated by the release of a starting gate and terminated by breakage of a “Goal” detector. The rat must pass its head through the opening and maintain a still posture with head at the midline for 1 second, upon which an instruction tone is issued. An ultrasound motion detector is used to monitor head and trunk movements (Gardiner and Kitai, 1992). In the cued task, a 1-kHz or 8-kHz tone (75 dB) is issued, instructing the rat to turn left or right, and terminating upon breakage of a “Goal” detector. In the delayed alternation task, a brief, low-volume 1-kHz tone is used to instruct the rat to make a head turn. Before a training session is initiated, juice is run through the spouts to equalize any olfactory cues. Trials are run in everyday light, with the experimental chamber surrounded by a Faraday cage lined with black paper. A videocamera is mounted to monitor and acquire a visual record of subjects’ behavior.

In neuronal recording experiments, the computer which controls the release of the starting gate, tone initiation and reinforcement delivery and records detector breakages sends messages to the acquisition computers when these events occur, triggering annotation of the neuronal data

stream. The behavioral video is juxtaposed with the timestamps of the acquisition software by means of a video mixer. Initiation of the starting posture (“Start”) must be determined by examination of timestamped behavioral video.

*Pretraining for both tasks:* Pretraining procedures are not reported by (Gardiner and Kitai, 1992). Rats will be subject to pretraining sessions until they learn to put their heads into the 35-mm wide vertical slot and hold head and body still for 2 seconds.

*Training for cued head movement:* Training and acquisition schedules are not reported by (Gardiner and Kitai, 1992). Each subject receives one training session per day, consisting of 40-70 trials (to be determined), with half of the trials for each cue tone, presented in pseudorandom order. After a rat first achieves the 72.5% correct criterion for acquisition, training continues for an additional 7-10 days. Lesioned rats are trained for a comparable number of days. Movement of head or body before the cue tone is given will be scored as errors. Movement of body which occurs with a cued head turn will cause the trial to be scored as an error. Failure to move for 1 minute after cue initiation will be scored as an error.

*Training for delayed alternation head movement:* Each subject will receive one training session per day, consisting of 40-70 trials (to be determined). After a rat first achieves the 72.5% correct criterion for acquisition, training will continue for an additional 7-10 days. Lesioned rats are trained for a comparable number of days. Movement of head or body before the cue tone is given will be scored as errors. Movement of body which occurs with a cued head turn will cause the trial to be scored as an error. Failure to move for 1 minute after cue initiation will be scored as an error.

### **4.3.3 Aim 1: experiments 1, 3, 5**

Experiments 1, 3, and 5 seek to verify the presumed dependence of the cued-arm T-maze, lever-press, and head movement tasks on dorsolateral striatal function, and to establish control tasks which differ only in their learning and memory requirements. The experiments all share the same design and methods; experiment 1 examines the cued and delayed alternation T-maze tasks, experiment 3 examines the cued and delayed alternation lever-press tasks, and experiment 5 examines the cued and delayed alternation head movement tasks.

#### **4.3.3.1 Hypothesis**

Normal rats’ acquisition and performance of the cued tasks is mediated by a system (presumably responsible for stimulus-response learning) which includes dorsolateral striatum and is distinct from the visuospatial learning/working memory system associated with the hippocampus. Conversely, the corresponding delayed alternation tasks depend upon the hippocampal rather than striatal system.

#### **4.3.3.2 Design**

The hypothesis is tested by attempting to establish a double dissociation of hippocampal and dorsolateral striatal function in performance of the cued tasks and the corresponding delayed alternation tasks, which involve similar motor, sensory, and motivational characteristics but presumably different learning and memory processes. The cued task is expected to depend upon the ability to form stimulus-response associations (“rule” or “habit” learning), whereas delayed alternation is expected to depend upon working memory of the last choice made. S-R learning is

associated with a neural system that includes dorsolateral striatum, whereas working memory and visuospatial learning are associated with a hippocampal system.

The performance of rats with bilateral dorsolateral striatal lesions is compared to that of normal rats and rats with bilateral fimbria-fornix lesions in the cued and delayed alternation tasks. If fimbria-fornix lesions cause a deficit relative to normals and rats with striatal lesions on delayed alternation but not on the cued task, delayed alternation is confirmed as an appropriate control for the cued task in subsequent experiments, employing similar task parameters but differing in learning requirements. If striatal lesions then cause a deficit relative to normals and rats with fimbria-fornix lesions on the cued task but not delayed alternation, the deficit may be attributed to loss of the specific learning ability necessary for the cued task. The hypothesis may be disproven if delayed alternation is shown to be dependent on hippocampus but not striatum and subjects with striatal lesions do not show a deficit on the cued task versus delayed alternation.

#### *4.3.3.3 Methods*

*Subjects:* The subjects are all male Sprague-Dawley rats, weighing 300-350 g, individually housed and on a regular day-night cycle. The rats are divided into eight groups: sham-striatal-lesioned and sham-fimbria-fornix-lesioned trained on the cued task, sham-striatal-lesioned and sham-fimbria-fornix-lesioned trained on delayed alternation, striatal-lesioned trained on the cued task, striatal-lesioned trained on delayed alternation, fimbria-fornix-lesioned trained on the cued task, and fimbria-fornix-lesioned trained on delayed alternation.

*Surgery:* Rats are anesthetized and given NMDA lesions in dorsolateral striatum or dorsal hippocampus according to the method of (Yin et al., 2004). After the rat is fixed in a stereotaxic frame with skull flat, 28-gauge cannulae are lowered bilaterally into the brain and 0.6 microliters of NMDA solution (0.12 M) is infused for a 3-minute period. The cannulae are removed after five more minutes. The striatal group has cannulae implanted at stereotaxic coordinates of AP = +0.7 mm, ML =  $\pm 3.6$  mm relative to bregma, and DV = -5 mm relative to skull surface. The hippocampal group has cannulae implanted at coordinates AP = -2.8 and -4.2 mm, ML =  $\pm 1.6$  and  $\pm 2.6$  mm relative to bregma, and DV = -4.3 and -4.0 mm relative to skull surface (Quinn et al., 2002). Two sham lesion groups (one at the hippocampal and one at the striatal coordinates) are subject to the same procedure, with the exception of NMDA infusion. Afterward, animals are slightly deprived of water and maintained at 85% of their normal body weight.

*Histology:* Following training, all lesioned animals will be deeply anesthetized and perfused. Brains will be fixed, sectioned, mounted, and stained with thionin as in (Yin et al., 2004) to analyze the extent of lesions without respect to behavioral performance.

*Data analysis:* Throughout the daily training sessions, each session's percentage of correct trials is collected for each of the rats. To test how a lesion affects overall success on each of the two training tasks, the session scores are compared between lesion groups (striatal lesion, hippocampal lesion, sham striatal and sham hippocampal lesions). A two-way 1-repeated measures ANOVA with one factor being the lesion group, the other factor being the session number and the independent variable being the session score, will be used to analyze the data from the cued and delayed alternation tasks separately. A main effect for lesion group is expected, as an indication of the involvement of the lesioned brain region, and a main effect for

session number is expected, as an indication of overall learning taking place. Post-hoc t-tests will be used to further establish score ordering between lesion groups.

#### *4.3.3.4 Expected results*

A double dissociation will be established of hippocampal and dorsolateral striatal function in performance of the cued and delayed alternation tasks. This result will demonstrate that the learning component of the cued tasks (thought to be the formation of stimulus-response associations) is dependent upon dorsolateral striatum, and that the delayed alternation tasks are appropriate controls for the cued tasks to be used in subsequent experiments, involving similar sensory, motor, and motivational factors but distinct learning and memory requirements.

If a double dissociation is not demonstrated for the lever-press tasks, it may still be worthwhile to do a modified version of experiment 4A without comparison to a control task, using one rather than two levers as in the original experiment of (Carelli et al., 1997), but analyzing responses to “Begin Trial,” “Start,” “Action Onset,” “Goal,” and “Reinforcement” in analogy to experiment 2A as described in the experimental design for experiment 4A. This modified experiment would give the opportunity to observe and investigate activity related to the “Begin/Start” phases and/or the “Goal/Reinforcement” phases of the tasks, analogous to that reported by (Jog et al., 1999) but unreported by (Carelli et al., 1997). Similarly, if a double dissociation is not demonstrated for the head movement tasks, it may still be worthwhile to do experiment 6A without comparison to a control task.

#### *4.3.4 Aims 2 and 4: experiments 2A, 4A, 6A*

Experiments 2A, 4A and 6A seek to characterize how (medium spiny) neuronal activity in levels of dorsolateral striatum anterior to bregma changes in correlation with acquisition of the stimulus-response associations necessary for performance of the cued-arm T-maze, lever-press, and head movement tasks. The experiments share the same design and methods, apart from the task to be examined.

##### *4.3.4.1 Hypotheses*

(a) Acquisition of the cued-arm T-maze, cued-lever press and cued-head movement (S-R) tasks is correlated with activity changes of neuronal populations in dorsolateral striatum at anterior levels.

(b) S-R learning activity changes appear only in neurons responsive to cutaneous stimulation and passive manipulation of the involved body part (examined in experiments 4A and 6A).

##### *4.3.4.2 Design*

For each experiment, two groups of subjects will both have tetrodes implanted in the anterior dorsolateral striatum as in (Jog et al., 1999). One group will learn the cued task, while the other will learn the delayed alternation task, established by experiment 1, 3, or 5 as a control task which incorporates similar sensory, motor, and motivational elements with different learning requirements which are not dependent on striatum. Any neuronal activity changes occurring in parallel with acquisition of the cued task must be compared with neuronal activity related to delayed alternation in order to ascertain relationships to stimulus-response learning versus sensory, motor, or motivational factors. Additionally, any activity correlated with the “Start”



and “Goal” phases of the cued task after acquisition analogous to that reported by (Jog et al., 1999) but unreported by (Carelli et al., 1997) is further explored by: a) separately analyzing the opening of the starting gate and initiation of starting posture/locomotion (“Begin Trial” versus “Start”), and varying the intertrial intervals; and b) separately analyzing the achievement of the maze goal and the reception of reinforcement (“Goal” versus “Reinforcement”), and varying the time of reinforcement delivery and the magnitude of reinforcement.

The implantation site will be very slightly shifted from (Jog et al., 1999) to record from the center of the area of striatum necessary for implementation of the instinctive four-phase grooming sequence (Cromwell and Berridge, 1996). Both the implantation site of (Jog et al., 1999) and the center of the “grooming area” of striatum identified by (Cromwell and Berridge, 1996) receive inputs from the same body part representations of primary motor and somatosensory cortices. Shifting the location of tetrode implantation will allow the demonstration of the involvement of this roughly 1 cubic millimeter of tissue in the performance of learned actions as well as instinctive sequences.

For the lever-press tasks and the head movement tasks only (experiments 4A and 6A), within each rat, two anterior tetrodes will be lowered to a functionally identified “left forelimb” area, and the other two tetrodes will be lowered to a functionally identified “neck” area. Changes of neuronal responsivity which parallel acquisition of the cued tasks may thus be compared between the two areas.

#### *4.3.4.3 Methods*

*Subjects:* The subjects are all male Sprague-Dawley rats, weighing 300-350 g, individually housed and on a regular day-night cycle. The rats are divided into two groups: cued task versus delayed alternation controls.

*Recording protocol:* Eight tetrodes manufactured and installed in a reusable drive according to the method of (Jog et al., 2002) and sections 3.2 and 3.3 will be independently lowered into the right striatum, four anteriorly and four posteriorly to bregma. (Experiments 2B, 4B, and 6B address the analysis of signals recorded at the posterior site.) Tetrodes will not be advanced over the course of training and recording sessions. Drives may be manufactured to allow dual-site recording as alluded to in (Jog et al., 2002). Preamplification, amplification, digitization, spike capture and storage, and unit isolation are implemented as described in sections 3.2 and 3.3. In order to record neuronal activity during reinforcement periods, an additional tetrode will be lowered into white matter to be used as a reference for differential recording.

*Surgery:* Subjects are anesthetized with 3 mL of 1.0 cc ketamine and 0.2 cc xylazine in 10 cc saline administered intraperitoneally and secured in a stereotaxic frame adjusted with skull flat. After opening the scalp, securing the skin and muscles back with clips, and stopping bleeders, eight or nine holes are drilled in the skull for installation of brass anchor screws. One of the screws will have a stainless steel wire wrapped around it for use as a ground wire. Once the anchor screws are installed, two holes are drilled at the sites for tetrode installation and dura is removed. The anterior site is AP = +0.7, ML = +3.5 mm (right striatum) with tetrodes lowered to approximately DV = -4.0 mm below dura. This is the center of an approximately 1 cubic millimeter volume of tissue determined by (Cromwell and Berridge, 1996) to be necessary for implementation of an instinctive four-phase grooming sequence. These coordinates are slightly altered from those used in (Jog et al., 1999) of AP = +0.5, ML = +3.7 mm, which would still fall

within the boundaries of this grooming area and receive inputs from the same group of body part representations in motor and somatosensory cortex (McGeorge and Faull, 1989). The posterior site is AP = -0.7, ML = +3.5 mm relative to bregma, which are the coordinates used by (Gardiner and Kitai, 1992) in the study of neuronal responses to a learned stimulus-response habit. The tetrode drive is positioned so that the cannulae holding the tetrodes at each site are within the opening just above the surface of the brain; the openings are sealed with bone wax and the skull surface and anchor screws are covered with dental acrylic to anchor the drive. The scalp is sutured with 4-0 nylon. After surgery, the rats are allowed to recover for a few days to relieve brain swelling before gradual advancement of tetrodes into the striatum. After reattainment of presurgical body weight, subjects are slightly deprived of water and maintained at 85% of that weight.

Additionally, two flexible 7-stranded EMG electrodes (A-M systems) will be installed by the method of (Carelli et al., 1997) in the biceps or triceps muscles of the left forelimb of subjects in the lever-press task and in the sternomastoid or cleomastoid muscles on each side of the neck of subjects in the head movement task, to obtain multiunit recordings which will allow accurate determination of movement onset times and to examine qualitative changes in EMG activity over acquisition of the tasks. The EMG electrodes may be joined up with the headstage connector to send signals through the preamplification, amplification, and digitization stages. The filters on the amplifier channels may be programmed to pass a bandwidth of 350-5000 Hz, as in (Carelli et al., 1997).

*Identification of neck and forelimb areas (experiments 4A and 6A only):* Groups of neck and forelimb-responsive neurons are identified in awake animals using the methods of (Cho and West, 1997; West, 1998). Tetrodes are advanced by small increments (e.g., 50 microns) and at each position, the responsiveness of neurons is tested by cutaneous stimulation and passive manipulation of 14 body part areas: ipsilateral and contralateral forelimbs, hindlimbs, vibrissae, shoulders and trunk, with the remaining four categories as head, neck, snout, and oral region (lip, chin, tongue). (Cho and West, 1997; West, 1998) have previously found that neuronal activity at a single site is responsive to one and only one body part. Cutaneous stimulation is delivered using a tapping probe and light stroking movements. Passive manipulation mimicks natural movement. (Carelli et al., 1997) conduct the identification tests with the rat “at rest” in the experimental chamber, behind the black blocking wall. Alternatively, the rat could be positioned in a restrainer (e.g., Braintree Scientific Universal Restrainer) to facilitate isolation of body parts for testing (Brown et al., 2002). Responsiveness of neurons is determined by listening to the audio record of firing while testing each body part. Two tetrodes will be centered (depth-wise) in a region responsive to left forelimb movements, and two will be centered in a neck-responsive region. The responsiveness of neurons around the tetrodes to the desired body parts will be verified daily before commencement of training sessions.

*Histology:* Before perfusion, each animal is deeply anesthetized and lesioned to mark the final positions of the tetrodes. The existing lesioning protocol involves bipolar pulse stimulation, 100 microamps for 2 minutes total duration, 4 pulses per second (Jog et al., 1998). The animal is then perfused, the brain removed, fixated, and cut into 25-micron sections, and stained with Nissl and cresyl violet for identification of lesions under light microscopy. In the current series of experiments it is of interest to register tetrode locations with respect to the striosome and matrix compartments; thus the stimulation and staining protocols may need to be modified to produce more compact lesions (on the order of, or smaller than, striosomes).

The protocol for staining lesions which mark tetrode positions must be compatible not only with the method for compartmental staining (see experiments 2C, 4C, and 6C) but also with anatomical identification of body part areas (see experiments 4D and 6D). If necessary, alternating slices may be stained for tetrode lesions, striosomal boundaries, and body part areas and then registered by some method.

The left forelimb of each animal is dissected to confirm the muscular innervation of the EMG electrodes.

*Data analysis:* For each rat, the percentage of units that show significant activity in a 1-second window centered on a task event is recorded for each event. Significant activity in a unit is defined as falling outside a 95% Poisson confidence interval established relative to a mean baseline firing rate for five consecutive 10-ms bins. Mean baseline firing rates for each unit are computed across all trials in a session from 300-ms periods of activity gathered at some interval before each trial begins (Jog et al., 1999).

Nine stages of training are defined to normalize behavioral data across rats. Stages 1-2 correspond to the first two sessions, stage 3 corresponds to the session when a rat first reaches the criterion for behavioral acquisition (defined as 72.5% trials correct), and stages 4-9 correspond to the next six sessions with scores above criterion performance (Jog et al., 1999).

The percentage of units responsive to each event is averaged for each stage over all rats in a group. For each group, whether or not an increase or decrease in the percentage of units responsive to a particular event between training stages is significant is tested using the  $\chi^2$  statistic at the 0.05 significance level. Changes that are found to be significant in the cued task group but also significant (and in the same direction) in the delayed alternation group cannot be correlated with stimulus-response acquisition. Directional specificity of responses will also be noted, as a method of distinguishing choice-specific responses from responses due to constant environmental factors; for example, responses which take place at one goal but not the other do not seem likely to be due to reinforcement consumption or anticipation.

Activity of individual neurons will be tracked over as many days as possible, as described in section 3.5.4, in order to determine to what extent the population recorded from remains stable over the training period, and whether activity changes over the learning period which are observed for the whole neuronal population are observable within individual neurons.

For experiments 4 and 6, data analysis will use the recordings from cued and delayed alternation groups from the areas of striatum that represent the involved body part (left forelimb in experiment 4 and neck in experiment 6). But for those experiments, data will also be gathered from an area representing a body part that is not involved in the task (neck in experiment 4 and left forelimb in experiment 6). The hypothesis that the neuronal activity changes correlated with stimulus-response acquisition only appear in the involved body part areas will be supported if no significant activity changes are found in the uninvolved body part areas.

To examine the effect of varying the intertrial interval, time of reinforcement delivery, and magnitude of reinforcement on post-acquisition activity at the "Begin Trial," "Start," "Goal," and "Reinforcement" events, activity from two additional sessions will be recorded, in which each subject will experience a single variation of one of the parameters. One rat will experience no change in parameter values for the two additional sessions as a control. The  $\chi^2$  statistic will be used to test for any significant decrease or increase in neuronal recruitment within each rat for

the extra sessions. Any significant change that is found in a rat experiencing a variation of a parameter but is not found in the control rat may be interpreted as correlated with the change in parameter value. Particular attention will be paid to the amount of "Goal"-related activity in the rats experiencing a different reinforcement delay and a different magnitude of reinforcement, and to the amount of "Begin" and "Start"-related activity in the rats experiencing a different magnitude of reinforcement and a different intertrial interval.

The effect of changes in intertrial interval, time of reinforcement delivery, and magnitude of reinforcement on neurons responsive to task events will be further explored using a within-neuron analysis. For each task event, the mean firing rate (spikes/s) and the mean peak response time offset (from the task event time) of each responding neuron are calculated over the 40 trials in the rat's last regular session (before the parameter value was changed). These means are then compared, neuron by neuron, to the means calculated from the final 40 trials conducted with the changed parameter value. Each pair of means is compared using a 2-tailed t-test at the 0.05 significance level. The percentage of neurons that show a significant change in firing rate and/or in peak response time offset with variation of parameter values will be reported.

#### *4.3.4.4 Expected results*

Sensorimotor activity (related to the "action" events) will disappear over the course of acquisition of the cued tasks, as in (Carelli et al., 1997; Jog et al., 1999). Activity related to the "Start" and "Goal" events in (Jog et al., 1999) may prove to be dependent upon parameters related to reinforcement delivery, reinforcement anticipation, or memory of recent reinforcement. Some of the "Goal" activity may signal the end of learned motor responses (Fujii and Graybiel, 2003). Such activity may not be observed for the cued lever-press and head-movement tasks, because reinforcement-responsive neurons may be located in striosomes, which are by definition not recorded from in experiments 4A and 6A.

Neuronal activity related to acquisition of the S-R tasks will appear only in units responsive to cutaneous stimulation and passive manipulation of the involved body part.

#### *4.3.5 Aims 3 and 4: experiments 2B, 4B, 6B*

##### *4.3.5.1 Hypotheses*

(a) Acquisition of the cued-arm T-maze, cued-lever press and cued-head movement (S-R) tasks is correlated with an increase in representation of the motor response in dorsolateral sensorimotor striatum at levels posterior to bregma.

(b) S-R learning activity changes appear only in units responsive to cutaneous stimulation and passive manipulation of the involved body part (examined in experiments 4B and 6B).

##### *4.3.5.2 Design*

Neuronal data from posterior levels of dorsolateral striatum is gathered simultaneously with data from anterior levels which is analyzed in experiments 2A, 4A, and 6A. Four tetrodes are lowered into the striatum at stereotaxic coordinates of AP = -0.7, ML = + 3.5 mm relative to bregma, which are the coordinates used in (Gardiner and Kitai, 1992) for study of neuronal responses to a learned stimulus-response habit. The tetrodes are lowered to approximately DV = -4.0 mm relative to skull surface and are not moved over the course of recording. In the lever-

press task and the head movement task, two tetrodes will be used to record from a forelimb area, and two from a neck area, the analysis focusing on the relevant body part area with the uninvolved area used as a control as in experiments 4A and 6A.

The systematization of implantation sites between tasks and of ML and (rough) DV coordinates between anterior and posterior sites will help to control for whether different medial or ventral extents of recording sites produced the different results of (Gardiner and Kitai, 1992) with respect to (Jog et al., 1999) and (Carelli et al., 1997).

#### *4.3.5.3 Methods*

*Data analysis:* For the posterior recordings, significant event-related changes in neuronal recruitment between training stages for the cued versus delayed alternation groups (and the involved versus uninvolved body part areas) are noted as in experiments 2A, 4A, and 6A. The profiles of significant changes between training stages for anterior and posterior areas can then be plotted for visual comparison. The Pearson's correlation coefficient will be calculated to test for a direct or inverse correlation between the changes of neuronal recruitment over the course of stimulus-response acquisition in the anterior and posterior areas within subjects.

*Histology:* The mediolateral positions of the anterior and posterior tetrodes will be compared to examine whether differences in position along this axis might account for any differences in experimental results.

#### *4.3.5.4 Expected results*

Sensorimotor activity (related to turning, lever press and head movement in experiments 2, 4, and 6) may appear at posterior levels of dorsolateral striatum as it disappears at anterior levels over the course of acquisition of the cued tasks only in units responsive to cutaneous stimulation and passive manipulation of involved body parts. If an anterior/posterior dissociation of motor learning/motor performance is demonstrated, an explanation will have to be found by recording from lateral versus medial sites in dorsolateral striatum (separated in ML by, e.g., 0.5-1 mm) and/or searching for anatomical differences between areas of dorsolateral striatum anterior and posterior to bregma.

### **4.3.6 Aim 5: experiments 2C, 4C, 6C**

#### *4.3.6.1 Hypothesis*

Neurons which are responsive to sensorimotor parameters in the cued-arm T-maze task, cued lever-press task and cued head movement task are located in the matrix of dorsolateral striatum, whereas any neurons which are responsive to cue or reinforcement parameters are located in striosomes of the dorsolateral striatum.

#### *4.3.6.2 Design*

The brains of subjects from the cued task groups of parts A and B of experiments 2, 4, and 6 are stained to identify the locations of striosomes and matrix relative to the tetrode locations marked by lesions prior to sacrifice. If any neurons were found in the previous experiments to be

responsive to cue or reinforcement parameters of the cued task, the locations of tetrodes they were recorded from will be particularly noted in relation to compartmental boundaries.

#### *4.3.6.3 Methods*

*Histology:* Before sacrifice and perfusion, tetrode positions will be marked by lesions as described in experiments 2A, 4A, and 6A. Brains will be removed, fixated, and sliced into 25-micron sections. If Nissl and cresyl violet staining to identify lesion locations are compatible with techniques of compartmental staining to be applied subsequently, every relevant slice may be treated with both techniques. Otherwise, alternate slices may be treated with each technique. Although staining for calbindin is one of the original and more popular methods for identifying striosomes (which appear as calbindin-poor patches), dorsolateral striatum is generally poor in calbindin and it is difficult to identify striosomes there by this method (White and Hiroi, 1998; Brown et al., 2002). Instead, compartments will be identified by staining with antiserum against the C-terminal peptide of the mu opiate receptor, after the method of (Canales and Graybiel, 2000).

*Data analysis:* Brain slices will be examined via light microscopy to determine the relationship of tetrode locations to striosomes and matrix without respect to the types of neurons recorded at each site. If lesion and compartmental staining must be carried out on alternating sections, adjacent slices will have to be registered in some fashion to allow superimposition of compartments over lesion locations. For lesions located squarely in matrix, this registration is unlikely to introduce error in compartmental identification. For lesions located in or on the borders of striosomes, some error may be introduced. Once tetrode relationships to striosomal borders have been registered, the locations of tetrodes from which cue or reinforcement-related neurons have been recorded will be identified.

#### *4.3.6.4 Expected results*

Lesions marking the positions of tetrodes which recorded from neurons responsive to the motor aspects of the task will be located in the matrix. Lesions marking the positions of tetrodes which recorded from neurons responsive to motor and to non-motor aspects of the task will straddle striosomal/matrix boundaries.

### **4.3.7 Aim 6: experiments 4D and 6D**

#### *4.3.7.1 Hypothesis*

Forelimb and neck areas defined by cutaneous stimulation and passive manipulation are in register with forelimb and neck areas defined by tracing anatomical connections between primary motor cortex and striatum.

#### *4.3.7.2 Design*

Small extracellular injections of an anatomical tracer will be made in the left forelimb or neck areas of cerebral cortex in rats which have acquired the cued tasks of experiments 4 and 6. After sacrifice, the rats' brains will be examined to determine the correspondence of patches stained anterogradely in striatum with lesions marking the positions of tetrodes which recorded from functionally identified forelimb and neck neurons in those animals.

#### 4.3.7.3 Methods

*Tracer injections:* Half of the rats will receive injections in the left forelimb area of primary motor cortex after recordings are concluded but before tetrode lesions are made; the other half will receive injections in the neck area of primary motor cortex. Small extracellular injections of biotinylated dextran amine (BDA) to trace axonal arborizations of corticostriatal neurons will be made using the method of (Kincaid et al., 1998; Hoover et al., 2003). A glass micropipette with a tip diameter of 20-40 microns is filled with a solution of 5% BDA in isotonic saline buffered with 0.01 M phosphate buffer and placed 1-2 mm from the surface of the appropriate area of motor cortex of the anesthetized animal. BDA is injected with a train of 5 mA current pulses lasting 7 seconds presented at intervals of 17 seconds over a 10-30 minute period. After 7-12 days, the animals are lesioned, anesthetized, perfused, and the brains are fixed and sliced for histological analysis. Identification of motor cortical neck and forelimb areas is guided by the mapping results from (Neafsey et al., 1986).

*Histology:* Brains are sliced into 25-micron sections and slices are treated with Nissl stain and cresyl violet to stain tetrode lesions (see experiments 2A, 4A, and 6A), and the antiserum for peptide C of the mu opiate receptor to find striosomal boundaries (see experiments 2C, 4C, and 6C). Treatments may be carried out on the same slices or on alternate slices. Additionally, the same or alternate slices are treated by the method of (Kincaid et al., 1998) for visualization of BDA. The sections are incubated for 2 hours in ABC solution, containing 0.2% Triton X-100, washed in buffered saline, and reacted for 10-20 minutes in a solution of 0.05% diaminobenzidine, 0.003% hydrogen peroxide, and 0.12% nickel chloride in buffered isotonic saline.

*Data Analysis:* Brain slices will be examined via light microscopy to determine the relationship of tetrode locations to neck and forelimb areas marked by tracing corticostriatal inputs from motor cortex with BDA without respect to the functional correlates of units recorded on tetrodes. If lesion, compartmental staining, and/or BDA visualization must be carried out on alternating sections, adjacent slices will have to be registered in some fashion to allow superimposition of stained body part areas over lesion locations.

#### 4.3.7.4 Expected results

Forelimb and neck areas in striatum identified by tracing with BDA from primary motor cortex will be in register with forelimb and neck neurons identified by electrophysiological recording and cutaneous stimulation/passive movement. As BDA traces the arborization of the corticostriatal projections, BDA-identified limb areas in striatum are likely to be slightly larger than would be identified by mapping neurons responsive to cutaneous stimulation/passive movement. The outlying parts of a particular arborization likely synapse onto medium spiny neurons which are predominantly innervated by other sets of inputs, and are therefore not usually responsive to stimulation by those outlying axonal branches.

#### 4.3.8 Aim 7: experiments 7A, 8A, 9A

##### 4.3.8.1 Hypothesis

Acquisition of the cued-arm T-maze, cued-lever press and cued-head movement (S-R) tasks is correlated with activity changes of neuronal populations in GPi.

#### 4.3.8.2 Design

Two groups of subjects will have tetrodes implanted in the GPi. One group will learn the cued task, while the other will learn the delayed alternation task, established previously as a control task which incorporates similar sensory, motor, and motivational elements with different learning requirements which are not dependent on striatum. Any neuronal activity changes occurring in parallel with acquisition of the cued task must be compared with neuronal activity related to delayed alternation in order to ascertain relationships to stimulus-response learning versus sensory, motor, or motivational factors.

#### 4.3.8.3 Methods

*Subjects, recording method, surgery, histology, task apparatus and procedures and pretraining and training protocols* are as for experiments 2A, 4A and 6A, with the exception of the tetrode implantation site.

*Tetrode implantation site:* Four tetrodes will be independently lowered into the GPi at stereotaxic coordinates ML = +3.5 mm, AP = -0.7 mm relative to bregma (Gardiner and Kitai, 1992).

*Data Analysis:* For each rat the percentage of units that show significant activity in a 1-second window centered on a task event is recorded for each event. Significant activity of a unit is defined as in experiments 2, 4, and 6. The percentage of units responsive to each event is averaged for each stage over all rats in a group. For each group, whether or not an increase or decrease in the percentage of units responsive to a particular event between training stages is significant will be tested using the  $\chi^2$  statistic at the 0.05 significance level. Changes that are found significant in the cued task but not in the delayed alternation task can be assumed to be correlated to stimulus-response acquisition.

#### 4.3.8.4 Expected results

If activity changes related to the acquisition or performance of learned stimulus-response habits exist in basal ganglia output areas, it is likely that these experiments will find activity related to all three cued tasks in GPi, which in primates has been observed to have neurons responsive to trunk and limb movements (Georgopoulos et al., 1983; Mink, 1996).

### 4.3.9 Aim 7: experiments 7B, 8B, 9B

#### 4.3.9.1 Hypothesis

Acquisition of the cued-arm T-maze, cued-lever press and cued-head movement (S-R) tasks is correlated with activity changes of neuronal populations in SNr.

#### 4.3.9.2 Design

Neuronal data from SNr is gathered simultaneously with data from GPi which is analyzed in part A of experiments 7, 8, and 9.



#### 4.3.9.3 Methods

*Tetrode implantation site:* Four tetrodes will be independently lowered into the SNr at stereotaxic coordinates ML = +3.5 mm, AP = -1.9 mm, and DV = -5.4 mm relative to bregma (Meyer-Luehmann et al., 2002).

#### 4.3.9.4 Expected results

If activity changes related to the acquisition or performance of learned stimulus-response habits exist in basal ganglia output areas, these experiments may not find such activity in SNr, which in primates has been observed to have neurons responsive to orofacial but not trunk and limb movements (DeLong et al., 1983).

### 4.4 Suggestions for further work

Completion of the proposed series of experiments would add to our understanding of how neuronal activity in dorsolateral striatum of rodents changes in correlation with learning of motor responses. Furthermore, the work begins to explore mappings between motor learning correlates of neuronal activity and the anatomical structure of striatum. Once this general framework is chalked out, several avenues of specific inquiry emerge (in addition to those which come from unanticipated results). The neuronal data already collected can be examined for how latency of significant firing responses to task events changes or doesn't change over S-R learning, or whether cross-correlations between neurons responsive to the same task events evolve over the course of learning. Perhaps other within-neuron or across-neuron features (see section 3.4) might be found in relation to task events, or to other aspects of behavior during the tasks. New versions of the cued tasks could include no-movement trials as in (Gardiner and Kitai, 1992) to pinpoint context-specificity in behavioral responses. Also, the dependence of the cued lever press and head movement tasks on S-R learning should be verified. Experiments 3 and 5 will most likely confirm the tasks' dependence on dorsolateral striatum, but whether task performance depends on acquisition of an S-R "habit" may be tested by looking for persistence of responses in intact vs. dorsolateral striatum-lesioned rats when reinforcement is devalued by pairing with lithium chloride injections, or by setting up probe trials to assess place versus response learning (DeCoteau et al., 2000; Yin et al., 2004).

Tetrodes' increased yield of units in local groups will be useful in investigating other questions raised by the anatomy of the corticostriatal and striatopallidal projections. The full range of types of stimulation and/or parameters of motor behavior to which body part-responsive neurons react, as well as what interactions occur between local groups of neurons responsive to the same body part (Cho and West, 1997), and how the response properties of these local groups (which presumably correspond to anatomically-defined body part areas) might be altered by functional reorganization of the primary motor cortex, are all large open questions. Furthermore, tetrodes would be useful in elucidating properties of functional topography in GPi and SNr, which might reflect on the nature of convergence of striatal input to basal ganglia output areas.

Finally, tasks which are more clearly analogous to procedural learning tasks in humans could be developed and the correlated neuronal behavior observed with tetrodes. A rodent version of the serial reaction-time task was discussed in section 4.1 (Christie and Dalrymple-Alford, 2004). It might also be possible to develop a version of probabilistic classification for rodents, involving the probabilistic relation of a small set of cues to one of two levers. Both of these tasks might be

called “visuomotor,” which suggests the placement of tetrodes to record activity in dorsomedial striatum in addition to dorsolateral striatum, allowing more inroads to be made in distinguishing the functions of these areas.

## **5 Conclusion**

Use of tetrodes in hippocampus of awake, freely behaving rodents has allowed investigators to examine behavioral correlates of firing patterns of large numbers of neurons (Wilson and McNaughton, 1993, 1994). In striatum, the technique has the additional potential to characterize the ensemble dynamics of local groups of neurons which are on the spatial scale of striosomes and matrisomes/body part representations, allowing the mapping of neuronal activity in those features to aspects of behavior. Progress has been made in improving the ease and robustness of tetrode manufacture and implantation, and the accuracy of unit separation and location reconstruction, which will likely lead in coming years to the widespread adoption of this preparation by researchers to record extracellular electrophysiological activity throughout the brain.

## Appendix: Finding $c$ , the spatial reconstruction parameter

The solution vector  $\mathbf{r}$  is parameterized by  $c$ :

$$\mathbf{r} = \frac{c\bar{\mathbf{A}}^{-1}\mathbf{p} + \bar{\mathbf{A}}^{-1}\Delta}{2}, \text{ where } \frac{c}{S_0} = |\mathbf{r}|^2.$$

Substituting  $\mathbf{r}$  into the equation for  $c$ :

$$\frac{c}{S_0} = \frac{1}{4} |c\bar{\mathbf{A}}^{-1}\mathbf{p} + \bar{\mathbf{A}}^{-1}\Delta|^2$$

Defining  $\boldsymbol{\alpha} = \bar{\mathbf{A}}^{-1}\mathbf{p}$  and  $\boldsymbol{\beta} = \bar{\mathbf{A}}^{-1}\Delta$ :

$$\begin{aligned} \frac{c}{S_0} &= \frac{1}{4} |c\boldsymbol{\alpha} + \boldsymbol{\beta}|^2 \\ &= \frac{1}{4} [(c\alpha_x + \beta_x)^2 + (c\alpha_y + \beta_y)^2 + (c\alpha_z + \beta_z)^2]; \end{aligned}$$

$$\frac{4c}{S_0} = c^2(\alpha_x^2 + \alpha_y^2 + \alpha_z^2) + 2c(\alpha_x\beta_x + \alpha_y\beta_y + \alpha_z\beta_z) + (\beta_x^2 + \beta_y^2 + \beta_z^2).$$

Defining  $\theta = \alpha_x^2 + \alpha_y^2 + \alpha_z^2$ ,  $\phi = \alpha_x\beta_x + \alpha_y\beta_y + \alpha_z\beta_z$ , and  $\gamma = \beta_x^2 + \beta_y^2 + \beta_z^2$ ,

$$\theta c^2 + 2(\phi - \frac{2}{S_0})c + \gamma = 0.$$

It is obvious that both  $\theta$  and  $\phi$  must be greater than zero.

## References

- Akins P.T., Surmeier D.J., Kitai S.T. (1990) Muscarinic modulation of the transient potassium current in rat neostriatal neurons. *Nature* 344:240-242.
- Aldridge J.W., Berridge K.C. (1998) Coding of serial order by neostriatal neurons: a "natural action" approach to movement sequence. *J.Neurosci.* 18:2777-2787.
- Alexander G.E., DeLong M.R. (1985) Microstimulation of the primate neostriatum. II. Somatotopic organization of striatal microexcitable zones and their relation to neuronal response properties. *J.Neurophysiol.* 53:1417-1430.
- Alexander G.E., Crutcher M.D. (1990) Functional architecture of basal ganglia circuits: neural substrates of parallel processing. *TINS* 13:266-271.
- Aosaki T., Kimura M., Graybiel A.M. (1995) Temporal and spatial characteristics of tonically active neurons of the primate's striatum. *J.Neurophysiol.* 73:1234-1252.
- Aosaki T., Tsubokawa H., Ishida A., Watanabe K., Graybiel A.M., Kimura M. (1994) Responses of tonically active neurons in the primate's striatum undergo systematic changes during behavioral sensorimotor conditioning. *J.Neurosci.* 14:3969-3984.
- Bennett B.D., Wilson C.J. (1998) Synaptic regulation of action potential timing in neostriatal cholinergic interneurons. *J.Neurosci.* 18:8539-8549.
- Bennett B.D., Callaway J.C., Wilson C.J. (2000) Intrinsic membrane properties underlying spontaneous tonic firing in neostriatal cholinergic interneurons. *J.Neurosci.* 20:8493-8503.
- Berridge K.C. (1989) Progressive degradation of serial grooming chains by descending decerebration. *Behav. Brain Res.* 33:241-253.
- Bishop C.M. (1995) *Neural Networks for Pattern Recognition*. New York: Oxford University Press.
- Brown L.L. (1992) Somatotopic organization in rat striatum: evidence for a combinational map. *Proc. Natl. Acad. Sci. USA* 89:7403-7407.
- Brown L.L., Sharp F.R. (1995) Metabolic mapping of rat striatum: somatotopic organization of sensorimotor activity. *Brain Res.* 686:207-222.
- Brown L.L., Smith D.M., Goldbloom L.M. (1998) Organizing principles of cortical integration in the rat neostriatum: corticostriate map of the body surface is an ordered lattice of curved laminae and radial points. *J.Compar.Neurol.* 392:468-488.
- Brown L.L., Feldman S.M., Smith D.M., Cavanaugh J.R., Ackermann R.F., Graybiel A.M. (2002) Differential metabolic activity in the striosome and matrix compartments of the rat striatum during natural behaviors. *J.Neurosci.* 22:305-314.
- Canales J.J., Graybiel A.M. (2000) A measure of striatal function predicts motor stereotypy. *Nat. Neurosci.* 3:377-383.

- Carelli R.M., Wolske M., West M.O. (1997) Loss of lever press-related firing of rat striatal forelimb neurons after repeated sessions in a lever pressing task. *J.Neurosci.* 17:1804-1814.
- Cho J., West M.O. (1997) Distributions of single neurons related to body parts in the lateral striatum of the rat. *Brain Res.* 756:241-246.
- Christie M.A., Dalrymple-Alford J.C. (2004) A new rat model of the human serial reaction time task: contrasting effects of caudate and hippocampal lesions. *J.Neurosci.* 24:1034-1039.
- Cromwell H.C., Berridge K.C. (1996) Implementation of action sequences by a neostriatal site: a lesion mapping study of grooming syntax. *J.Neurosci.* 16:3444-3458.
- Crutcher M.D., Alexander G.E. (1990) Movement-related neuronal activity selectively coding either direction or muscle pattern in three motor areas of the monkey. *J.Neurophysiol.* 64:151-163.
- DeCoteau W.E., Hu D., Kubota Y., Graybiel A.M. (2000) Striatal lesions impair performance of a T-maze procedural learning task in rats. *Soc. Neurosci. Abstr.* 26:254.19.
- DeLong M.R., Crutcher M.D., Georgopoulos A.P. (1983) Relations between movement and single cell discharge in the substantia nigra of the behaving monkey. *J.Neurosci.* 3:1599-1606.
- Djurfeldt M., Kubota Y., Hu D., DeCoteau W.E., Graybiel A.M. (2001) Patterned correlated activity in the rat sensorimotor striatum during learning of a T-maze task. *Soc. Neurosci. Abstr.* 27:514.10.
- Doyon J., Owen A.M., Petrides M., Sziklas V., Evans A.C. (1996) Functional anatomy of visuomotor skill learning in human subjects examined with positron emission tomography. *Eur. J. Neurosci.* 8:637-648.
- Eblen F., Graybiel A.M. (1995) Highly restricted origin of prefrontal cortical inputs to striosomes in the macaque monkey. *J.Neurosci.* 15:5999-6013.
- Fee M.S., Mitra P.P., Kleinfeld D. (1996a) Automatic sorting of multiple unit neuronal signals in the presence of anisotropic and non-Gaussian variability. *J.Neurosci. Methods* 69:175-188.
- Fee M.S., Mitra P.P., Kleinfeld D. (1996b) Variability of extracellular spike waveforms of cortical neurons. *J.Neurophysiol.* 76:3823-3833.
- Flaherty A.W., Graybiel A.M. (1991) Corticostriatal transformations in the primate somatosensory system. Projections from physiologically mapped body-part representations. *J.Neurophysiol.* 66:1249-1263.
- Flaherty A.W., Graybiel A.M. (1993a) Output architecture of the primate putamen. *J.Neurosci.* 13:3222-3237.
- Flaherty A.W., Graybiel A.M. (1993b) Two input systems for body representation in the primate striatal matrix: Experimental evidence in the squirrel monkey. *J.Neurosci.* 13:1120-1137.
- Flaherty A.W., Graybiel A.M. (1994) Input-output organization of the primate sensorimotor striatum. *J.Neurosci.* 14:599-610.

- Fujii N., Graybiel A.M. (2003) Representation of action sequence boundaries by macaque prefrontal cortical neurons. *Science* 301:1246-1249.
- Gardiner T.W., Kitai S.T. (1992) Single-unit activity in the globus pallidus and neostriatum of the rat during performance of a trained head movement. *Exp. Brain Res.* 88:517-530.
- Georgopoulos A.P., DeLong M.R., Crutcher M.D. (1983) Relations between parameters of step-tracking movements and single cell discharge in the globus pallidus and subthalamic nucleus of the behaving monkey. *J.Neurosci.* 3:1586-1598.
- Gerfen C.R. (1992) The neostriatal mosaic: multiple levels of compartmental organization in the basal ganglia. *Annu. Rev. Neurosci.* 15:285-320.
- Gray C.M., Maldonado P.E., Wilson M., McNaughton B. (1995) Tetrodes markedly improve the reliability and yield of multiple single-unit isolation from multi-unit recordings in cat striate cortex. *J.Neurosci. Methods* 63:43-54.
- Graybiel A.M. (1990) Neurotransmitters and neuromodulators in the basal ganglia. *TINS* 13:244-254.
- Graybiel A.M. (1998) The basal ganglia and chunking of action repertoires. *Neurobiol. Learn. Mem.* 70:119-136.
- Groves P.M., Linder J.C., Young S.J. (1994) 5-hydroxydopamine-labeled dopaminergic axons: three-dimensional reconstructions of axons, synapses and postsynaptic targets in rat neostriatum. *Neuroscience* 58:593-604.
- Groves P.M., Garcia-Munoz M., Linder J.C., Manley M.S., Martone M.E., Young S.J. (1995) *Elements of the intrinsic organization and information processing in the neostriatum*. In: Models of Information Processing in the Basal Ganglia (Houk JC, Davis JL, Beiser DG, eds), pp 51-83. Cambridge, MA: MIT Press.
- Harris K.D., Henze D.A., Csicsvari J., Hirase H., Buzsaki G. (2000) Accuracy of tetrode spike separation as determined by simultaneous intracellular and extracellular measurements. *J.Neurophysiol.* 84:401-414.
- Hazrati L.N., Parent A. (1992) The striatopallidal projection displays a high degree of anatomical specificity in the primate. *Brain Res.* 592:213-227.
- Henze D.A., Borhegyi Z., Csicsvari J., Mamiya A., Harris K.D., Buzsaki G. (2000) Intracellular features predicted by extracellular recordings in the hippocampus in vivo. *J.Neurophysiol.* 84:390-400.
- Hikosaka O., Sakamoto M., Usui S. (1989) Functional properties of monkey caudate neurons. I. Activities related to saccadic eye movements. *J.Neurophysiol.* 61:780-798.
- Hoover J.E., Hoffer Z.S., Alloway K.D. (2003) Projections from primary somatosensory cortex to the neostriatum: the role of somatotopic continuity in corticostriatal convergence. *J.Neurophysiol.* 89:1576-1587.
- Hu D., Kubota Y., Graybiel A.M. (2001) Successive resculpting of task-related activity patterns in the striatum during action-sequence procedural learning, extinction and relearning. *Soc. Neurosci. Abstr.* 27:514.9.

- Jog M.S., Connolly C.I., Hillegaart V., Wilson M.A., Graybiel A.M. (1996) Multiunit tetrode recording in rat striatum. *Soc. Neurosci. Abstr.* 22.
- Jog M.S., Kubota Y., Connolly C.I., Iyengar D.R., Graybiel A.M. (1997) Behavior related ensemble activity in striatum of rats. *Soc. Neurosci. Abstr.* 23:464.
- Jog M.S., Connolly C.I., Kubota Y., Iyengar D.R., Graybiel A.M. (1998) Methods for tetrode calibration, implantation, neuroimaging, and analysis of multiunit recordings in striatum. *Soc. Neurosci. Abstr.* 24:649.11.
- Jog M.S., Kubota Y., Connolly C.I., Hillegaart V., Graybiel A.M. (1999) Building neural representations of habits. *Science* 286:1745-1749.
- Jog M.S., Connolly C.I., Kubota Y., Iyengar D.R., Garrido L., Harlan R., Graybiel A.M. (2002) Tetrode technology: advances in implantable hardware, neuroimaging, and data analysis techniques. *J.Neurosci. Methods* 117:141-152.
- Jueptner M., Weiller C. (1998) A review of differences between basal ganglia and cerebellar control of movements as revealed by functional imaging studies. *Brain* 121:1437-1449.
- Jueptner M., Frith C.D., Brooks D.J., Frackowiak R.S.J., Passingham R.E. (1997) Anatomy of motor learning. II. Subcortical structures and learning by trial and error. *J.Neurophysiol.* 77:1325-1337.
- Kawaguchi Y. (1993) Physiological, morphological, and histochemical characterization of three classes of interneurons in rat neostriatum. *J.Neurosci.* 13:4908-4923.
- Kawaguchi Y. (1997) Neostriatal cell subtypes and their functional roles. *Neurosci. Res.* 27:1-8.
- Kawaguchi Y., Wilson C.J., Emson P.C. (1990) Projection subtypes of rat neostriatal matrix cells revealed by intracellular injection of biocytin. *J.Neurosci.* 10:3421-3438.
- Kawaguchi Y., Wilson C.J., Augood S.J., Emson P.C. (1995) Striatal interneurons: chemical, physiological and morphological characterization. *TINS* 18:527-535.
- Kermadi I., Joseph J.P. (1995) Activity in the caudate nucleus of monkey during spatial sequencing. *J.Neurophysiol.* 74:911-933.
- Kimura M. (1990) Behaviorally contingent property of movement-related activity of the primate putamen. *J.Neurophysiol.* 63:1277-1296.
- Kimura M., Kato M., Shimazaki H., Watanabe K., Matsumoto N. (1996) Neural information transferred from the putamen to the globus pallidus during learned movement in the monkey. *J.Neurophysiol.* 76:3771-3786.
- Kincaid A.E., Zheng T., Wilson C.J. (1998) Connectivity and convergence of single corticostriatal axons. *J.Neurosci.* 18:4722-4731.
- Kjartansson V. Assistant Professor, Department of Electrical Engineering, University of Iceland, Reykjavik.
- Knowlton B.J., Squire L.R., Gluck M.A. (1994) Probabilistic category learning in amnesia. *Learn. Mem.* 1:106-120.
- Koos T., Tepper J.M. (1999) Inhibitory control of neostriatal projection neurons by GABAergic interneurons. *Nature Neuroscience* 2:467-472.

- Kubota Y., Kawaguchi Y. (1993) Spatial distributions of chemically identified intrinsic neurons in relation to patch and matrix compartments of rat neostriatum. *J.Compar.Neurol.* 332:499-513.
- Kubota Y., Hu D., DeCoteau W.E., Harlan R., Graybiel A.M. (2000) Multi-neuronal activity in mouse striatum recorded chronically during T-maze learning. *Soc. Neurosci. Abstr.* 26:683.
- Laforce R., Doyon J. (2001) Distinct contribution of the striatum and cerebellum to motor learning. *Brain Cogn.* 45:189-211.
- Lewicki M.S. (1994) Bayesian modeling and classification of neural signals. *Neural Comp.* 6:1005-1030.
- Liles S.L., Updyke B.V. (1985) Projections of the digit and wrist area of precentral gyrus to the putamen: relation between topography and physiological properties of neurons in the putamen. *Brain Res.* 339:245-255.
- Maillard L., Ishii K., Bushara K., Waldvogel D., Schulman A.E., Hallett M. (2000) Mapping the basal ganglia: fMRI evidence for somatotopic representation of face, hand, and foot. *Neurology* 55:377-383.
- Matsumoto N., Minamimoto T., Graybiel A.M., Kimura M. (2001) Neurons in the thalamic CM-Pf complex supply striatal neurons with information about behaviorally significant sensory events. *J.Neurophysiol.* 85:960-976.
- McGeorge A.J., Faull R.L.M. (1989) The organization of the projection from the cerebral cortex to the striatum in the rat. *Neuroscience* 29:503-537.
- Meyer-Luehmann M., Thompson J.F., Berridge K.C., Aldridge J.W. (2002) Substantia nigra pars reticulata neurons code initiation of a serial pattern: implications for natural action sequences and sequential disorders. *Eur. J. Neurosci.* 16:1599-1608.
- Mink J.W. (1996) The basal ganglia: focused selection and inhibition of competing motor programs. *Prog. Neurobiol.* 50:381-425.
- Miyachi S., Hikosaka O., Lu X. (2002) Differential activation of monkey striatal neurons in the early and late stages of procedural learning. *Exp. Brain Res.* 146:122-126.
- Miyachi S., Hikosaka O., Miyashita K., Karadi Z., Rand M.K. (1997) Differential roles of monkey striatum in learning of sequential hand movement. *Exp. Brain Res.* 115:1-5.
- Nadasdy Z. (1998) Spatio-temporal patterns in the extracellular recording of hippocampal pyramidal cells: from single spikes to spike sequences. Ph.D. Thesis. Department of Neuroscience, Rutgers, the State University of New Jersey.
- Nambu A., Yoshida S., Jinnai K. (1990) Discharge patterns of pallidal neurons with input from various cortical areas during movement in the monkey. *Brain Res.* 519:183-191.
- Neafsey E.J., Bold E.L., Haas G., Hurley-Gius K.M., Quirk G., Sievert C.F., Terreberry R.R. (1986) The organization of the rat motor cortex: a microstimulation mapping study. *Brain Res. Rev.* 11:77-96.



- Oorschot D.E. (1996) Total number of neurons in the neostriatal, pallidal, subthalamic, and substantia nigral nuclei of the rat basal ganglia: a stereological study using the Cavalieri and optical disector methods. *J. Comp. Neurol.* 366:580-599.
- Packard M.G., McGaugh J.L. (1992) Double dissociation of fornix and caudate nucleus lesions on acquisition of two water maze tasks: further evidence for multiple memory systems. *Behav. Neurosci.* 106:439-446.
- Packard M.G., McGaugh J.L. (1996) Inactivation of hippocampus or caudate nucleus with lidocaine differentially affects expression of place and response learning. *Neurobiol. Learn. Mem.* 65:65-72.
- Packard M.G., Hirsh R., White N.M. (1989) Differential effects of fornix and caudate nucleus lesions on two radial maze tasks: evidence for multiple memory systems. *J. Neurosci.* 9:1465-1472.
- Parent A. (1990) Extrinsic connections of the basal ganglia. *TINS* 13:254-258.
- Parent A., Levesque M., Parent M. (2001) A re-evaluation of the current model of the basal ganglia. *Parkinsonism and Related Disorders* 7:193-198.
- Plenz D., Kitai S.T. (1998) Up and down states in striatal medium spiny neurons simultaneously recorded with spontaneous activity in fast-spiking interneurons studied in cortex-striatum-substantia nigra organotypic cultures. *J. Neurosci.* 18:266-283.
- Quirk M.C., Wilson M.A. (1999) Interaction between spike waveform classification and temporal sequence detection. *J. Neurosci. Methods* 94:41-52.
- Ragozzino M.E. (2003) Acetylcholine actions in the dorsomedial striatum support flexible shifting of response patterns. *Neurobiol. Learn. Mem.* 80:257-267.
- Ragozzino M.E., Jih J., Tzavos A. (2002) Involvement of the dorsomedial striatum in behavioral flexibility: role of muscarinic cholinergic receptors. *Brain Res.* 953:205-214.
- Rall W. (1962) Electrophysiology of a dendritic neuron model. *Biophys. J.* 2:145-167.
- Rauch S.L., Whalen P.J., Savage C.R., Curran T., Kendrick A., Brown H.D., Bush G., Breiter H.C., Rosen B.R. (1997) Striatal recruitment during an implicit sequence learning task as measured by functional magnetic resonance imaging. *Hum. Brain Mapp.* 5:124-132.
- Romo R., Scarnati E., Schultz W. (1992) Role of primate basal ganglia and frontal cortex in the internal generation of movements. II. Movement-related activity in the anterior striatum. *Exp. Brain Res.* 91:385-395.
- Sakamoto T., Okaichi H. (2001) Use of win-stay and win-shift strategies in place and cue tasks by medial caudate putamen (MCPu) lesioned rats. *Neurobiol. Learn. Mem.* 76:192-208.
- Schmitzer-Torbert N., Redish A.D. (2004) Neuronal activity in the rodent dorsal striatum in sequential navigation: separation of spatial and reward responses on the multiple T task. *J. Neurophysiol.* Epub ahead of print.
- Schultz W., Romo R. (1992) Role of primate basal ganglia and frontal cortex in the internal generation of movements. I. Preparatory activity in the anterior striatum. *Exp. Brain Res.* 91:363-384.

- Schultz W., Apicella P., Romo R., Scarnati E. (1995) *Context-dependent activity in primate striatum reflecting past and future behavioral events*. In: Models of Information Processing in the Basal Ganglia (Houk JC, Davis JL, Beiser DG, eds), pp 11-27. Cambridge, MA: MIT Press.
- Takahashi S., Anzai Y., Sakurai Y. (2003) Automatic sorting for multi-neuronal activity recorded with tetrodes in the presence of overlapping spikes. *J.Neurophysiol.* 89:2245-2258.
- Tanji J., Shima K., Mushiake H. (1996) Multiple cortical motor areas and temporal sequencing of movements. *Brain Res. Cogn. Brain Res.* 5:117-122.
- Thompson R. (1978) *A Behavioral Atlas of the Rat Brain*. New York: Oxford University Press.
- Tunstall M.J., Oorschot D.E., Kean A., Wickens J.R. (2002) Inhibitory interactions between spiny projection neurons in the rat striatum. *J.Neurophysiol.* 88:1263-1269.
- West M.O. (1998) Anesthetics eliminate somatosensory-evoked discharges of neurons in the somatotopically organized sensorimotor striatum of the rat. *J.Neurosci.* 18:9055-9068.
- White N.M., Hiroi N. (1998) Preferential localization of self-stimulation sites in striosomes/patches in the rat striatum. *Proc. Natl. Acad. Sci. USA* 95:6486-6491.
- Wickens J.R., Wilson C.J. (1998) Regulation of action-potential firing in spiny neurons of the rat neostriatum in vivo. *J.Neurophysiol.* 79:2358-2364.
- Wilson C.J. (1995) *The contribution of cortical neurons to the firing pattern of medium spiny neurons*. In: Models of Information Processing in the Basal Ganglia (Houk JC, Davis JL, Beiser DG, eds), pp 29-50. Cambridge, MA: MIT Press.
- Wilson M.A., McNaughton B.L. (1993) Dynamics of the hippocampal ensemble code for space. *Science* 261:1055-1058.
- Wilson M.A., McNaughton B.L. (1994) Reactivation of hippocampal ensemble memories during sleep. *Science* 265:676-679.
- Yin H.H., Knowlton B.J., Balleine B.W. (2004) Lesions of dorsolateral striatum preserve outcome expectancy but disrupt habit formation in instrumental learning. *Eur. J. Neurosci.* 19:181-189.
- Zheng T., Wilson C.J. (2002) Corticostriatal combinatorics: the implications of corticostriatal axonal arborizations. *J.Neurophysiol.* 87:1007-1017.